Ecological Modelling 319 (2016) 233–254

Contents lists available at ScienceDirect

Ecological Modelling

journal homepage: www.elsevier.com/locate/ecolmodel

Analysing the spatial and temporal dynamics of species interactions in mixed-species forests and the effects of stand density using the 3-PG model

David I. Forrester[a,*], Xiaolu Tang[b]

[a] Chair of Silviculture, Faculty of Environment and Natural Resources, Freiburg University, Tennenbacherstr. 4, 79108, Freiburg, Germany
[b] Chair of Forest Inventory and Remote Sensing, Georg-August-Universität Göttingen, Büsgenweg 5, 37077, Göttingen, Germany

ARTICLE INFO

Article history:
Received 16 May 2015
Received in revised form 9 July 2015
Accepted 14 July 2015
Available online 30 July 2015

Keywords:
Biodiversity
Biomass
Complementarity
Forest growth model

ABSTRACT

The growth dynamics and ecosystem services from mixed-species stands are often difficult to predict because the way a given combination of species interacts changes as resource availability or climatic conditions change from site to site or as stands develop over time. Empirical data for many of these situations is often nonexistent. The forest growth model 3-PG was adapted for mixed-species forests and for thinned stands by modifying the light-absorption routine and allowing for within-canopy vertical gradients in climate in the water balance routine. It was also adapted for deciduous species and to predict diameter distributions. The resulting model, 3-PG_{mix}, was used to examine the growth dynamics of subtropical mixed-species forests containing *Castanopsis sclerophylla*, *Cunninghamia lanceolata* and *Liquidambar formosana*, with a wide range of stand densities in Shitai County, Anhui Province, China. After parameterizing and calibrating 3-PG_{mix} using data from monocultures, its predictions of leaf and stem biomass, basal area and light absorption by each species within the mixture were highly correlated with measured values. 3-PG_{mix} also predicted spatial and temporal changes in complementarity, expressed as the relative differences in growth of a given species in mixture compared with its monoculture. Complementarity was predicted to change as the stands developed, across gradients in fertility and rainfall, and also at different stand densities. Such information could be used to suggest potential species compositions, species proportions and thinning regimes for new mixed-species plantations or the responses of existing mixtures to changes in species proportions, stand density and climate. 3-PG is widely used as a routine management tool for monospecific stands and this study shows that it could potentially be used for mixed-species stands as well.

1. Introduction

Mixed-species forests can be more productive than monocultures when complementary traits and species interactions enable them to use a higher proportion of the sites resources or to use them more efficiently. However, mixtures are certainly not always more productive than monocultures. A given combination of species can be more productive than monocultures on some sites or ages but less productive elsewhere (Forrester, 2014a). This is because the interactions between species changes spatially and temporally with changes in resource availability or climatic conditions (Forrester, 2014a). Species interactions can also be modified by differences in stand density (Garber and Maguire, 2004; Amoroso and Turnblom, 2006; Condés et al., 2013) and probably also by management activities or disturbances that influence density. To make the most of these interactions and to determine how to manage forests under changing management and climatic conditions, tools that can predict these spatial and temporal dynamics and disturbance effects are required.

There are countless combinations of species, silvicultural treatments, soil and climatic conditions in any given region. In many cases, foresters are interested in combinations of these variables that may not currently exist, especially when the goal is to establish new mixed-species plantations. Traditional empirical growth and yield models often unrealistically assume stable site conditions (Battaglia and Sands, 1998). In some tree-level models inter-specific interactions are estimated from empirical relationships based on competition indices calculated from the size of, or shading from, neighbouring trees (Peng, 2000; Pretzsch et al., 2015). These empirical relationships often require large data sets

* Corresponding author. Tel.: +49 761 203 8628.
E-mail address: david.forrester@waldbau.uni-freiburg.de (D.I. Forrester).

http://dx.doi.org/10.1016/j.ecolmodel.2015.07.010
0304-3800/

to develop and are restricted to the stand structures or site and climatic conditions represented in the data set (Battaglia and Sands, 1998; Peng, 2000; Landsberg, 2003). This is because they do not consider the main factors that influence forest growth including resource availability, climatic conditions or different silvicultural regimes (Korzukhin et al., 1996; Monserud, 2003). On the other hand, models that are based on general and fundamental ecophysiological processes can potentially provide robust extrapolations to untested conditions, silvicultural regimes (Weiskittel et al., 2010) and species combinations and proportions. While some important physiological processes work at high temporal (seconds, hours) or spatial (leaves, trees) resolutions, models that operate at these resolutions often require detailed and expensive physiological data to parameterise and validate (Battaglia and Sands, 1998). Calculations at high resolutions can also lead to errors that are propagated when upscaling, and are not necessary when the desired outputs are at lower temporal (months or years) or spatial (stands) resolutions, such as those often required by forest managers.

In an attempt to bridge the gap between conventional empirical models and process-based models, hybrid models have been developed to capture some of the advantages of both (Landsberg and Waring, 1997; Battaglia and Sands, 1998; Sands and Landsberg, 2002; Landsberg, 2003; Härkönen et al., 2010; Landsberg and Sands, 2010; Weiskittel et al., 2010). These include the generality and ability of process-based models to describe the forests' interaction with its environment and hence its response to changes in environmental conditions and management (Battaglia and Sands, 1998). In addition, complex physiological relationships can be replaced with simpler and lower resolution (and sometimes more empirical) relationships. This can reduce data input and parameterisation requirements and provide outputs at the desired resolution without any need to scale up. In some cases, the hybrid models provide even better growth predictions than empirical models developed for the same regions, probably partly because they account for intra- and inter-annual climatic variability (Weiskittel et al., 2010; Pérez-Cruzado et al., 2011).

The forest growth model 3-PG (Physiological Principles Predicting Growth) is an example of such a model. It is a simple process-based (or hybrid) model that has been widely used and well validated for all the processes it considers, such as growth, biomass partitioning, light absorption, water balance, responses to CO_2, diameter distributions and mortality (Landsberg and Sands, 2010). It is widely used in South America as a management tool to complement routine inventory and strategic planning (Landsberg, 2003; Almeida et al., 2004b; Battaglia et al., 2007). It has been incorporated into a decision support system to assess plantation water yield and productivity in South Africa (Dye, 2005) and into the FullCam model for carbon accounting of Australian forests (Paul et al., 2006). Many more examples are described in Landsberg and Sands (2010). This wide-spread use is unusual for a process-based model and reflects its simple and transparent structure, the feasible input requirements, the relatively easily testable outputs for each process that it models, and importantly, the fact that it has always been freely available and well documented (Landsberg and Sands, 2010).

The 3-PG model was developed for even-aged monocultures and the aim of this study was to modify 3-PG so that it could be used to examine the growth dynamics of each species within a mixed-species forest and their responses to disturbances that modify stand density, such as thinning. The 3-PG model was chosen because no other models with comparable simplicity could be found that have been so rigorously tested in terms of observed-predicted comparisons for all of their component processes in so many different types of forests. In addition, to reproduce the spatial and temporal dynamics of species interactions in mixtures, models probably need to account for the physiological functioning of the trees, the environmental conditions within the stand, the stand structure, and interactions between these, as well as the external influences of climate and disturbances (Pretzsch et al., 2015). These components are all included in 3-PG or could be added with minor modifications. This was done for subtropical forests containing *Castanopsis sclerophylla, Cunninghamia lanceolata, Cyclobalanopsis glauca* and *Liquidambar formosana*, with a wide range of stand densities in Shitai County, Anhui Province, China. Mixed-species plantations of the same or related species have also been considered in Southern China (Meng et al., 2014). Specifically, the objectives were (1) to convert 3-PG into a mixed-species model and parameterise it for these species, one of which is deciduous; (2) to calibrate it using monospecific stands and assess its performance when predicting mixed-species dynamics and (3) to examine the spatial and temporal dynamics of the interactions between these species.

2. Description of 3-PG

3-PG was developed by Landsberg and Waring (1997). A review of the 3-PG model, its calibration and validation and many examples of its application is in Landsberg and Sands (2010). 3-PG_{PJS} 2.7 (Sands, 2010) was used to develop the mixed-species version of 3-PG, 3-PG_{mix}, which can still be run as 3-PG_{PJS} 2.7. The 3-PG_{mix} model is described in detail in Appendix A. The following provides an overview of the model followed by the changes that were required for it to work in mixed-species forests, for deciduous species and in forests where the stand density is reduced. The parameters and their units are in Table 1.

The 3-PG model consists of five simple sub-models in a causal chain starting with light absorption and assimilation and ending with the conversion of biomass into output variables of interest to forest managers (Landsberg and Waring, 1997; Sands and Landsberg, 2002). These all work on a monthly time step. The first sub-model predicts light absorption and calculates gross primary production (GPP) based on the maximum potential light-use efficiency (α_{Cx}), which is reduced in response to limitations imposed by temperature, frost, vapour pressure deficit (VPD), soil moisture, soil fertility, atmospheric CO_2 and stand age (Landsberg and Waring, 1997; Sands and Landsberg, 2002; Almeida et al., 2004a). Net primary production (NPP) is calculated assuming NPP/GPP = 0.47 (Waring et al., 1998). The second sub-model distributes the NPP to foliage, stems and roots. Partitioning to roots is influenced by soil fertility, VPD and soil moisture, and then partitioning between stem and foliage is influenced by tree size such that larger trees partition a lower proportion of NPP to foliage (Landsberg and Waring, 1997; Sands and Landsberg, 2002). The third sub-model determines whether there is any density-dependent mortality using the −3/2 self-thinning law and adjusts the number of trees per ha accordingly (Landsberg and Waring, 1997; Sands and Landsberg, 2002). It also calculates density independent mortality if required (Sands, 2004a; Gonzalez-Benecke et al., 2014). The fourth sub-model calculates the soil water balance. The canopy conductance g_c is calculated using a species-specific maximum g_c, leaf area index (L) and any limitations imposed by VPD, soil moisture, atmospheric CO_2 and stand age. This sub-model calculates transpiration (and soil evaporation) with the Penman–Monteith equation, which is added to the canopy interception to predict evaportranspiration. The soil water is calculated as the difference between evaportranspiration and rainfall and any water in excess of the maximum soil water holding capacity is drained off (Sands and Landsberg, 2002). When evapotranspiration is greater than the available soil water, the NPP is reduced accordingly. The fifth sub-model converts the biomass into output variables that are often of interest to forest managers, such as mean tree diameter, height, basal area, wood volume, etc.

Table 1
Description of parameters, their values, sources and when they are required. The "Source" column refers to "Default" values for *E. globulus* in 3-PG$_{PJS}$ 2.7, "Observed" values that were measured in this study or obtained from published observations, and "Fitted" values that were obtained as described in the text. Labels in the "When required" column refer to whether the parameter is required for any type of simulation (*) or whether it is only required when using the 3-PG$_{PJS}$ 2.7 light sub-model (L1), the new light sub-model (L2), or the new evapotranspiration calculations that consider within canopy VPD, net radiation and g_a gradients (E).

Parameter	Symbol	Units	Source	*Castanopsis sclerophylla*	*Cunninghamia lanceolata*	*Cyclobalanopsis glauca*	*Liquidambar formosana*	When required
Biomass partitioning and turnover								
Allometric relationships and partitioning								
Foliage:stem partitioning ratio at B = 2 cm	p_2	–	Fitted	0.80	0.75	0.90	0.40	*
Foliage:stem partitioning ratio at B = 20 cm	p_{20}	–	Fitted	0.50	0.60	0.50	0.15	*
Constant in the stem mass vs. B relationship	a_S	–	Observed	0.10	0.05	0.30	0.30	*
Power in the stem mass vs. B relationship	n_S	–	Observed	2.49	2.51	2.20	2.09	*
Maximum fraction of NPP to roots	η_{Rx}	–	Fitted	0.6	0.6	0.6	0.6	*
Minimum fraction of NPP to roots	η_{Rn}	–	Fitted	0.3	0.2	0.2	0.25	*
Litterfall and root turnover								
Maximum litterfall rate	γ_{Fx}	1/month	Observed	0.059	0.049	0.059	0.028	*
Litterfall rate at t = 0	γ_{F0}	1/month	Default	0.001	0.001	0.001	0.001	*
Age at which litterfall rate has median value	$t_{\gamma F}$	months	Observed	48	48	48	48	*
Average monthly root turnover rate	γ_R	1/month	Default	0.015	0.015	0.015	0.015	*
If deciduous, the month when leaves produced	leaf$_P$	month	Observed	0	0	0	2	
If deciduous, the month when leaves fall	leaf$_L$	month	Observed	0	0	0	11	
NPP and conductance modifiers								
Temperature modifier (f_T)								
Minimum temperature for growth	T_{min}	deg. C	Observed	0	0	5	0	*
Optimum temperature for growth	T_{opt}	deg. C	Observed	17.5	17.5	16	17.5	*
Maximum temperature for growth	T_{max}	deg. C	Observed	40	40	40	40	*
Frost modifier (f_F)								
Days production lost per frost day	k_F	days	Default	1	1	1	1	*
Soil water modifier (f_θ)								
Moisture ratio deficit for f_θ = 0.5	c_θ	–	Observed	0.7	0.7	0.7	0.7	*
Power of moisture ratio deficit	n_θ	–	Observed	9	9	9	9	*
Atmospheric CO_2 modifier (f_C)								
Assimilation enhancement factor at 700 ppm	$f_{C\alpha 700}$	–	NA	1	1	1	1	
Canopy conductance enhancement factor at 700 ppm	f_{Cg700}	–	NA	1	1	1	1	
Fertility effects								
Value of 'm' when FR = 0	m_0	–	Default	0	0	0	0	*
Value of 'f_N' when FR = 0	f_{N0}	–	Default	0.6	0.6	0.6	0.6	*
Power of (1-FR) in 'f_N'	n_{fN}	–	Default	1	1	1	1	*
Age modifier (f_{AGE})								
Maximum stand age used in age modifier	t_x	years	NA	200	200	200	200	*
Power of relative age in function for f_{AGE}	n_{age}	–	Default	4	4	4	4	*
Relative age to give f_{AGE} = 0.5	r_{age}	–	Default	0.95	0.95	0.95	0.95	*
Self-thinning								
Mortality rate for large t	γ_{Nx}	%/year	NA	0	0	0	0	
Seedling mortality rate (t = 0)	γ_{N0}	%/year	NA	0	0	0	0	
Age at which mortality rate has median value	$t_{\gamma N}$	years	NA	0	0	0	0	
Shape of mortality response	$n_{\gamma N}$	–	NA	1	1	1	1	
Max. stem mass per tree at 1000 trees/hectare	w_{Sx1000}	kg/tree	Default	300	300	300	300	*
Power in self-thinning rule	n_m	–	Default	1.5	1.5	1.5	1.5	*
Fraction mean single-tree foliage biomass lost per dead tree	m_F	–	Default	0	0	0	0	*
Fraction mean single-tree root biomass lost per dead tree	m_R	–	Default	0.2	0.2	0.2	0.2	*
Fraction mean single-tree stem biomass lost per dead tree	m_S	–	Default	0.2	0.2	0.2	0.2	*
Canopy structure and processes								
Specific leaf area								
Specific leaf area at age 0	σ_0	m^2/kg	Observed	12.6	7.1	16.2	16.0	*
Specific leaf area for mature leaves	σ_1	m^2/kg	Observed	6.5	5.5	6.5	12.0	*
Age at which specific leaf area = (SLA0 + SLA1)/2	t_σ	years	Observed	2	3	2	4	*
Light interception								
Extinction coefficient for absorption of PAR by canopy	k or k_H	–	Observed	0.66	0.29	0.54	0.65	*[b]
Age at canopy cover	t_c	years	Observed	3	3	3	3	L1
Maximum proportion of rainfall evaporated from canopy	I_{Rx}	–	Observed[f]	0.15	0.25	0.15	0.25	*
LAI for maximum rainfall interception	L_{Ix}	–	Observed	4	5	4	4	*
LAI for 50% reduction of VPD in canopy	L_{50D}	–	Default	5	5	5	5	E
Production and respiration								
Canopy quantum efficiency	α_{Cx}	molC/molPAR	Observed	0.027	0.042	0.039	0.020	*
Ratio NPP/GPP	Y	–	Default	0.47	0.47	0.47	0.47	*
Conductance								
Minimum canopy conductance	g_{Cmin}	m s^{-1}	Default	0	0	0	0	*
Maximum canopy conductance	g_{Cmax}	m s^{-1}	Default	0.02	0.02	0.02	0.02	*
LAI for maximum canopy conductance	L_{gCmax}	–	Default	3.33	3.33	3.33	3.33	*
Defines stomatal response to VPD	k_D	1/mBar	Default[e]	0.05	0.05	0.086	0.05	*
Canopy boundary layer conductance	g_B	m s^{-1}	Default	0.2	0.2	0.2	0.2	*

Table 1 (*Continued*)

Parameter	Symbol	Units	Source	*Castanopsis sclerophylla*	*Cunninghamia lanceolata*	*Cyclobalanopsis glauca*	*Liquidambar formosana*	When required
Wood $\delta^{13}C$ (Wei et al., 2014a,b)								
The ratio of diffusivities of CO_2 and water vapour in air	–	–	Default/NA	0.66	0.66	0.66	0.66	
$\delta^{13}C$ difference of modelled tissue and new photosynthate	ε_{sp}	per mil	Default/NA	2	2	2	2	
Fractionation against ^{13}C in diffusion	a	per mil	Default/NA	4.4	4.4	4.4	4.4	
Enzymatic fractionation by Rubisco	b	per mil	Default/NA	27	27	27	27	
Wood and stand properties								
Branch and bark fraction (p_{BB})								
Branch and bark fraction at age 0	p_{BB0}	–	NA	0.75	0.75	0.75	0.75	[c]
Branch and bark fraction for mature stands	p_{BB1}	–	NA	0.15	0.15	0.15	0.15	[c]
Age at which $p_{BB} = (p_{BB0} + p_{BB1})/2$	t_{BB}	years	NA	2	2	2	2	
Basic density								
Minimum basic density—for young trees	ρ_0	Mg/m^3	Observed[a]	0.53	0.35	0.66	0.48	[c]
Maximum basic density—for older trees	ρ_1	Mg/m^3	Observed[a]	0.53	0.35	0.66	0.48	[c]
Age at which $\rho = (\rho_0 + \rho_1)/2$	t_ρ	years	NA	1	1	1	1	[c]
Stem height								
Constant in the stem height relationship	a_H	–	Observed	1.77	2.01	2.68	3.79	L2, E
Power of B in the stem height relationship	n_{HB}	–	Observed	0.60	0.61	0.43	0.42	L2, E
Power of competition in the stem height relationship	n_{HC}	–	Observed	0	0	0	0	L2, E
Stem volume								
Constant in the stem volume relationship	a_V	–	Observed	0.000085	0.000078	0.00018	0.00014	*, L2[d]
Power of B in the stem volume relationship	n_{VB}	–	Observed	0	0	0	0	*, L2[d]
Power of height in the stem volume relationship	n_{VH}	–	Observed	0	0	0	0	*, L2[d]
Power of $B^2 \times$ height in the stem volume relationship	n_{VBH}	–	Observed	0.92	0.91	0.82	0.84	*, L2[d]
Crown shape								
Crown shape (1 = cone, 2 = ellipsoid, 3 = half-ellipsoid, 4 = rectangular)	–	–	Observed	3	3	3	3	L2, E
Crown diameter								
Constant in the crown diameter relationship	a_K	–	Observed	0.42	0.76	0.59	0.48	L2, E
Power of B in the crown diameter relationship	n_{KB}	–	Observed	0.91	0.58	0.82	0.98	L2, E
Power of height in the crown diameter relationship	n_{KH}	–	Observed	0	0	0	0	L2, E
Power of competition in the crown diameter relationship	n_{KC}	–	Observed	0	0	0	0	L2, E
Live-crown length								
Constant in the LCL relationship	a_{HL}	–	Observed	0.51	0.28	1.01	1.71	L2, E
Power of B in the LCL relationship	n_{HLB}	–	Observed	0.84	1.11	0.70	0.53	L2, E
Power of LAI in the LCL relationship	n_{HLL}	–	Observed	0	0	0	0	L2, E
Power of competition in the LCL relationship	n_{HLC}		Observed	0	0	0	0	L2, E
Diameter distributions[f]								
Constant for Weibull scale parameter of B dist.	sc_{B0}	–	Observed	10.10	7.26	7.92	9.01	
Constant in the Weibull shape parameter of B dist.	sh_{B0}	–	Observed	1.85	1.78	1.81	1.76	
Intercept of CV of B distribution vs age relationship	a_{BCV}	–	Observed	0.47	0.49	0.48	0.47	
Slope of CV of B distribution vs age relationship	b_{BCV}	–		0	0	0	0	
ws distributions[f]								
Constant in the Weibull scale parameter of w_s dist.	sc_{w0}	–	Observed	11.13	5.75	7.27	11.78	
Constant in the Weibull shape parameter of w_s dist.	sh_{w0}	–	Observed	1.45	1.53	1.41	2.26	
Intercept of CV of w_s distribution vs age relationship	a_{wCV}	–	Observed	0.54	0.45	0.57	0.51	
Slope of CV of w_s distribution vs age relationship	b_{wCV}	–	Observed	0	0	0	0	
Conversion factors								
Intercept of net vs. solar radiation relationship	Q_a	W/m^2	Default	0	0	0	0	*
Slope of net vs. solar radiation relationship	Q_b	–	Default	0.8	0.8	0.8	0.8	*
Molecular weight of dry matter		gDM/mol	Default	24	24	24	24	*
Conversion of solar radiation to PAR		mol/MJ	Default	2.3	2.3	2.3	2.3	*

[a] Includes bark.
[b] If using L2 this k needs to be for homogeneous canopies (k_H).
[c] Only required if no stem volume parameters are supplied or competition is used in allometric equations.
[d] Only required if no branch and bark fraction or basic density parameters are supplied.
[e] Default for all species except *C. glauca*, which is observed (Huang et al., 2011).
[f] Only the Weibull parameters that were used for this study are listed.

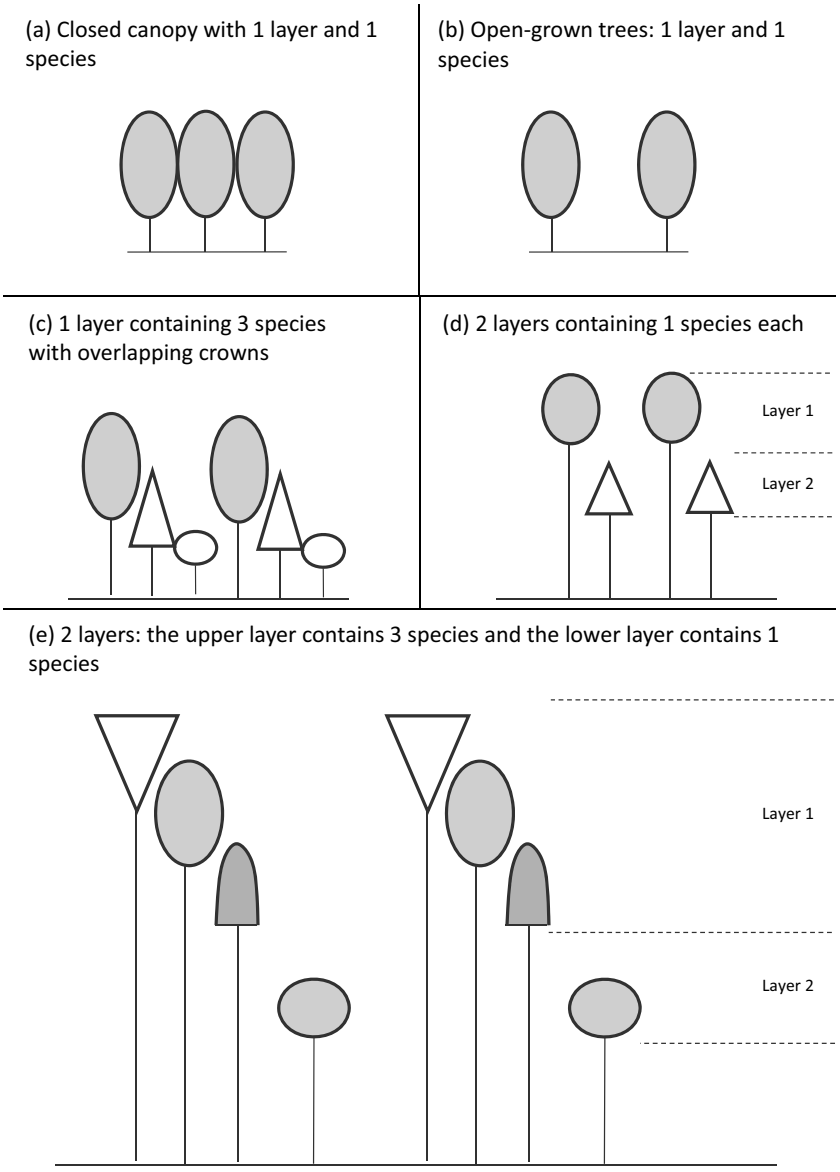

Fig. 1. Examples of the canopy structures that can be modelled using 3-PG$_{mix}$ including a closed (a) and open canopy (b) with only one species, or more complex canopies that contain multiple species and multiple layers (c–e). A single layer contains all species whose crowns overlap vertically. Modified from Forrester (2014b) and Forrester et al. (2014).

Several studies have applied 3-PG to predict the growth or transpiration of two-species mixtures (Feikema et al., 2010a; López-Serrano et al., 2015). These focused on a special type of mixture where one species overtops a second species with no vertical overlap between the crowns (Fig. 1d). This study aimed to develop 3-PG so that it could be used for mixtures with >two species, and also for mixtures with canopy structures where there is vertical overlap between the species, as well as densities ranging from open grown trees to closed canopies, and can therefore be used for all canopy structures shown in Fig. 1.

3. Changes made to produce 3-PG$_{mix}$

The modifications described below were made to 3-PG$_{PJS}$ 2.7, which is freely available as an Excel file at http://3pg.forestry.ubc.ca/. The 3-PG$_{mix}$ model is also freely available as an Excel file at the same web site.

3.1. Light absorption

The most significant modification comprised of three changes to the light absorption calculations. Previous versions of 3-PG used the Lambert-Beer law to calculate light absorption from *L*, a light extinction coefficient *k* and the canopy cover (option L1 in Table 1 and Appendix A). 3-PG$_{mix}$ also uses the Lambert-Beer law but required three changes (option L2 in Table 1 and Appendix A). Firstly, the earlier calculations will not work for mixed-species forests except the special case when they have a stratified canopy without any vertical overlap (Fig. 1d), and this is often not the case. A new light absorption model has been added to 3-PG$_{mix}$ that works for mixed-species forests with multiple canopy layers that can each contain several species (Fig. 1; Forrester, 2014b; Forrester et al., 2014).

Secondly, the original light model assumed that *k* is constant for a given species, however, *k* varies significantly with canopy structure and *L* (Binkley et al., 2013), such as with changes in age, site

quality and season (Cannell et al., 1987). Several studies have done sensitivity analyses of 3-PG and found that it can be sensitive to the k parameter, depending on the outputs examined (Esprey et al., 2004; Xenakis et al., 2008). This variability in k can be accounted for to some extent by replacing k with an extinction coefficient for a homogeneous (not heterogeneous, see Eq. (A.19)) canopy, k_H (Duursma and Mäkelä, 2007), and this was applied in the new light absorption sub-model of 3-PG$_{mix}$ (Forrester, 2014b; Forrester et al., 2014). This is described in detail in Appendix A.

Thirdly, to account for open canopies, such as young stands or thinned stands, the previous versions of 3-PG use a canopy cover value, ζ (between 0 and 1), that increases with stand age until the canopy closes. However, it does not account for disturbances that open the canopy after it has already closed and Gonzalez-Benecke et al. (2014) therefore used allometric equations that predict crown projection area from stem diameter to predict ζ when applying 3-PG to *Pinus elliottii* forests. However, while the ζ helps to account for the reduction in light absorption due to a reduction in leaf area, it may not adequately account for the simultaneous increase in individual tree light absorption due to a reduction in shading from neighbours. This can result in an underestimate of light absorption when the canopy is not closed (Forrester et al., 2014). The new light absorption sub-model does not use ζ and accounts for different canopy openness using an empirical constant that is a function of mean monthly midday solar zenith angle, k_H, the mean tree leaf area to crown surface area ratio and the proportion of the canopy volume that is filled with tree crowns (Forrester et al., 2014). More details are provided in Appendix A. The sub-model has been tested for a wide range of canopy structures in terms of species, mixed-species compositions and stand densities, including the forests used in this study.

It is important to note that while 3-PG$_{mix}$ allows for vertical heterogeneity such that species can differ in height (Fig. 1) it is assumed that there is no horizontal heterogeneity. That is, it assumes that that species are mixed tree-by-tree as opposed to row-by-row or group-by-group. It is therefore not designed to examine gap dynamics.

3.2. Vertical climatic gradients within the canopy

Species at different heights within the canopy of mixed-species forests could experience different microclimates. As shown in Fig. 1, the canopy structure in 3-PG$_{mix}$ is no longer a single "big leaf" as in the original version of 3-PG, and so vertical gradients in canopy microclimate may sometimes be significant. In addition to the vertical gradient in light availability, 3-PG$_{mix}$ also considers vertical gradients in aerodynamic conductance (g_a), VPD and net radiation. The g_a is modelled as a function of the g_a above the canopy and the height of the given species within the canopy (Appendix A). The VPD is a function of the VPD above the canopy and the L above the crowns of the given species (Appendix A). The net radiation is calculated assuming the same light extinction coefficients for photosynthetically active radiation as suggested by Wallace (1997) (Appendix A). Therefore, the net radiation used to predict transpiration varies with stand structure. This contrasts with the previous versions of 3-PG that predicted transpiration using the total net radiation, regardless of canopy cover, and therefore did not predict soil evaporation separately; all net radiation was used in a single evapotranspiration calculation. 3-PG$_{mix}$ uses all net radiation that was not absorbed by the trees to predict soil evaporation. Vertical gradients in radiation and VPD, as well as the separation of transpiration and soil evaporation, have also recently been added to a monospecific version of 3-PG with a detailed water balance (Almeida and Sands, 2015).

3.3. Accounting for species proportions

Several relationships in 3-PG depend on maximum values of L or the number of trees per ha (N). These are based on the L or N of monocultures and need to be adjusted in 3-PG$_{mix}$ so that the same equations can be used for mixtures (Eqs. (A.30), (A.35) and (A.39) in Appendix A). It is critical that the species proportions used are calculated using appropriate variables, and the variable that is most appropriate depends on the relationship. The L used to calculate canopy interception or canopy conductance is adjusted using species proportions based on their contribution to stand L. Whereas the N used for self-thinning calculations is adjusted based on the species proportions in terms of basal area; proportions in terms of N are not used because competition is more likely to be related to stand basal area (or biomass or leaf area) than the number of trees per ha; a single N could represent a wide range of basal areas.

3.4. Deciduous species

When deciduous species have lost their leaves it is assumed that they are dormant and have no NPP, respiration, transpiration or light absorption. This assumption may not be strictly true if there is respiration during the dormant season but these processes are assumed to be negligible. In 3-PG$_{mix}$, deciduous species require two additional parameters including the month when leaves are produced (leaf$_P$) and the month when they are lost (leaf$_L$). All leaves will be lost at the beginning of the leaf$_L$ month. The foliage biomass (W_F) that was lost at the start of leaf$_L$ will be produced again at the end of the month leaf$_P$. From the month leaf$_P$ all NPP will be partitioned to W_F (none to W_S or W_R) until an NPP equal to the W_F has been produced, and after that, NPP will be partitioned to W_S, W_R and W_F as usual. This assumption may be inappropriate, such that after the W_F of deciduous species is rebuilt there may not be much more NPP allocated to W_F for the rest of the growing season, and instead the NPP is allocated to W_S and W_R. However, this is currently not done in 3-PG$_{mix}$ because it would prevent any annual change in W_F and no data were available about the seasonality of biomass allocation. Only four studies could be found that applied 3-PG to deciduous species. Three of these, which modelled *Populus* hybrids and *Salix dasyclados*, modelled these species as if they were evergreen (Amichev et al., 2010, 2011; Headlee et al., 2013). In the fourth study the dormant period of *Betula platyphylla* was modelled using the 3-PG temperature modifier such that there was zero GPP during winter months with temperatures lower than a defined minimum (Potithep and Yasuoka, 2011). This is also possible in 3-PG$_{mix}$ but this will only stop the trees from functioning during the cold period. There will be no leaf loss and no assimilates will be required to rebuild the canopy in spring because the W_F was retained and simply becomes active again. This approach also assumes that the dormant period is only influenced by temperature, but other factors, such as water availability might also be important. The use of only leaf$_P$ and leaf$_L$ in 3-PG$_{mix}$ to define the growing season ignores the fact that W_F is not produced and lost instantly at the start or end of a month but builds up and is lost gradually over about one month or so (Norby et al., 2003). A less abrupt seasonal change in litterfall of evergreen species was considered in Gonzalez-Benecke et al. (2014) but was not implemented in 3-PG$_{mix}$ to maintain as much simplicity as possible.

3.5. Diameter distributions and bias corrections

Several allometric equations are used by 3-PG. Some of the predicted variables are only used as outputs (e.g. volume), while some are used for other calculations relating to various processes within 3-PG, such as the partitioning variable p_{FS} that is calculated from mean tree diameter (B) (Eq. (A.28) in Appendix A), or B which is

itself calculated from w_s (by inverting Eq. (A.65) in Appendix A). Most of these relationships are not linear and will lead to biased predictions of the given response variable due to Jensen's Inequality; the mean of a function is not the same as the function of the mean (Duursma and Robinson, 2003). This bias should be corrected to prevent its propagation through other calculations and is done in 3-PG$_{mix}$ following the approach of Duursma and Robinson (2003) and described in detail in Appendix A. This correction takes account of the coefficient of variation of the predictor variables, which can be provided as an input parameter or can be calculated from Weibull distributions of B or w_s that are described using empirical equations whose parameters are inputs (Appendix A). A similar approach for predicting diameter distributions in 3-PG was used by Landsberg et al. (2005). If required, these diameter distributions are used to provide outputs for a user-defined number of the largest-diameter trees per ha, such as the height of the largest 100 trees per ha as an estimate of mean dominant height, or the volume of the crop tree s (Appendix A).

4. Methods

4.1. Site description

Model predictions were compared with data collected from subtropical monospecific *Cunninghamia lanceolata* plantations that were about 14- to 20-years-old and monospecific and mixed-species forests containing *C. sclerophylla, C. lanceolata* and *L. formosana* that were about 16- to 42-years-old and located in Shitai County, Anhui Province, China (29°59′–30°24′N, 117°12′–117°59′E). The stands varied in terms of L from <1 to 10.2, trees per ha from 88 to 2741 and basal area from 1 to 57 m^2 ha^{-1}. In mixtures, the proportion of a given species varied from 5 to 94% in terms of basal area or 5 to 90% in terms of trees per ha. Mean annual precipitation is about 1410 mm, the monthly mean maximum and minimum temperatures in July are 32.9 °C and 25.9 °C, respectively, and in January are 7.4 °C and 1.0 °C, respectively (1951–2012). The topography includes level to steep slopes (up to 107%). Long-term average (1951–2012) climate data were obtained from the GHCN (Menne et al., 2012; NOAA, 2013), see also Appendix Fig. B.1. Long-term average data was used in simulations because there were missing data in 2005 and 2013.

4.2. Data collection and estimation of model parameters

A total of 43 plots were selected from an inventory based on 100 m × 100 m systematic grids (Tang, 2015). Plots were only selected for this study if they were even aged and if at least 90% of the basal area and trees per ha included the four species used for this study. The plots were circular. All trees within a radius of 6 m, with diameters (B) > 10 cm at 1.3 m, were measured for diameter. All those outside the 6 m radius but inside a 10 m radius, with B > 20 cm, were also measured for diameter. These diameter measurements were made between March and May 2013. The heights of one or two dominant trees, one co-dominant tree and one suppressed tree were also measured in each plot.

4.2.1. Biomass

To estimate above-ground biomass, volume and leaf area, allometric equations were developed using a total of 68 trees sampled within the 43 measurement plots (Guisasola, 2014). For each species present within a plot, one dominant, one co-dominant and one suppressed tree were sampled. In addition to the four focal species, one additional species, *Castanopsis eyrei* was included in the 68 sample trees because it was also present in some plots and was required to calculate stand attributes when <100% of the plot was composed of the four focal species of this study. The biomass sampling is described in detail in Guisasola (2014) and Guisasola et al. (2015) and follows the same procedure used in Forrester et al. (2012). After felling the tree, the diameters and heights of all branches were measured and three live branches (and additional dead branches, when present) per tree were sampled to develop allometric equations to predict branch biomass and branch leaf area. The leaves from these branches and those from seedlings in the same stand were used to estimate the specific leaf area parameters for young and older trees and their relationship with age (σ_0, σ_1, t_σ). The whole stem was weighed in the field and converted to a dry weight using a wet-to-dry weight ratio of wood discs that were sampled at 2-m intervals along the stem and dried at 100 °C to constant weight. The stem volume was calculated from diameter and bark thickness measurements at 0 m, 0.3 m, 1.3 m, 3 m and every 2 m thereafter. The live-crown length and the crown diameter were also measured on all 68 trees. Below-ground biomass was not measured in this study and was predicted using allometric equations from the literature (Xiang et al., 2011; Kang et al., 2012; Chen et al., 2013; He et al., 2013; Lai et al., 2013; Zeng, 2015).

4.2.2. Light absorption

The light absorption predictions by 3-PG$_{mix}$ were compared with those from a much more detailed tree-level model, Maestra (Medlyn, 2004). The Maestra light predictions compared well with field data in other mixed-species stands (Charbonnier et al., 2013; le Maire et al., 2013). Maestra accounts for shading from neighbouring trees using individual x- and y-coordinates of each tree. It accounts for differences in crown architecture in terms of crown shapes, crown length and width, leaf area, the vertical distribution of leaf-area density, the leaf angle distribution and the optical properties of leaves. The parameterisation of Maestra for these plots is described in detail in Forrester et al. (2014), which also calculated the extinction coefficient parameter (k_H) for these species and stands. These data were combined with data from four other experiments including mixtures and monocultures with a wide range of species, species compositions, species proportions and stand densities to develop the light sub-model used in 3-PG$_{mix}$ (see Forrester et al., 2014).

4.2.3. Quantum yield and biomass partitioning

The efficiency with which photosynthetically active radiation (PAR) is used to produce biomass (the canopy quantum efficiency, α) was estimated by determining the maximum growth rates of individual trees of a given species and then scaling this to the stand level using the trees per ha at the same age to create a hypothetical monospecific stand of individuals with this maximum growth rate. It was therefore assumed that these trees were not limited by temperature, frost, VPD, soil moisture or soil fertility. A preferable approach would be to have time series data from monospecific stands that are known to be non-limited by these factors (e.g., Almeida et al., 2004a), however these data were not available.

The maximum annual growth by individual trees of a given species was obtained from tree-ring analyses sampled from the same stands, including the same trees used for above-ground biomass measurements (Tang et al., in review). The diameters of these trees were then used to predict above-ground biomass increments using the allometric equations. Based on the inventory data, it was estimated that at the age of these maximum growth rates, there would have been about 2000 trees per ha, and this was used to predict stand level biomass and L at the same age. The stand density and crown architectures of the trees when growing at these maximum rates were used as input for the Maestra model to predict the annual absorption of PAR by these hypothetical monocultures.

Litterfall was predicted using values in the literature for stands with similar stand structures and growth rates (Chen et al., 2005; Zhao et al., 2009; Fan et al., 2013; Zhang et al., 2013). This was added

to the biomass growth to estimate NPP, and was also used to predict the maximum litterfall rate (γ_{Fx}). The age of maximum litterfall rate ($t_{\gamma F}$) was estimated to be one year after canopy closure. GPP was calculated from NPP assuming a ratio of NPP to GPP of 0.47. These data were then used to provide an estimate of the maximum α (α_{Cx}) for each species.

The temperature limits on α (T_{min}, T_{opt}, T_{max}) were approximations (based on Zhou and Gao, 1985; Liu, 2009; Zhang and Deng, 2009; Tang et al., 2014) and default frost effects ($k_F = 1$) were used. Parameters used by the age modifier were selected to remove any effects of age-related decline because the forests studied were relatively young (<50 years). Default values for the effects of vapour pressure deficit on α were used for each species except *C. glauca* for which k_D could be estimated from Huang et al. (2011). Default parameters for the fertility effects on α were also used. Direct empirical measurements of soil fertility were not available. The fertility rating (FR) for each monospecific plot was calculated, after all other parameters had been determined, by adjusting to an FR for a given location that gave satisfactory model performance for all monocultures (Landsberg et al., 2005). The FR for mixed-species plots was assumed to be the same as the FR of monospecific plots in the same forest area.

The foliage to stem partitioning parameters (p_2, p_{20}) and the minimum and maximum partitioning to roots (η_{Rx} and η_{Rn}) were "fitted" (Table 1) by varying these parameters until predicted and observed foliage, stem and root mass of monocultures were in agreement with the values estimated using the allometric equations in the monospecific plots.

4.2.4. Self-thinning

The management of these forests included frequent and low-intensity thinning and it was rare to observe dead trees. Therefore, no data could be obtained to estimate density-dependent or density-independent mortality parameters. Density-dependent mortality was avoided in simulations (that were compared with observed data) by including thinning in the simulations at regular intervals (and low intensities) down to the observed trees per ha at the time of plot measurements.

4.2.5. Size distributions

The scale and shape parameters of diameter (B) and stem mass (w_S) Weibull distributions were predicted for mean monospecific stands using the 43 measurement plots. Mean stands were used because the plot data did not show any age, stand density or species composition effects on the size distributions, although this probably would have been evident from a larger data set. The size distributions of a given species in mixed-species plots were converted to equivalent monospecific size distributions by dividing the trees per ha of each size class (for the given species) by the proportional contribution that species made to the total plot basal area. The scale and shape parameters were fitted to two-parameter right truncated Weibull distributions using the *fitdistrplus* package in R (Delignette-Muller et al., 2014). The location parameter was estimated by 3-PG$_{mix}$ as described in Appendix A. The coefficients of variation of the mean size distributions were also calculated.

4.2.6. Rainfall interception

The maximum proportion of rainfall intercepted by the canopy (I_{Rx}) of a given species monoculture was estimated from the literature while considering similar stand structures and species; *Castanopsis* and *Cyclobalanopsis* = (Xu et al., 2005), *C. lanceolata* = (Pan et al., 1989), *Liquidambar* = (Xiao and McPherson, 2011; Kirnbauer et al., 2013). The L for maximum rainfall interception (L_{Ix}) was predicted assuming that this L would be similar to that where the relationship between L and PAR absorption was close to its asymptote, which was estimated using the Maestra predictions of PAR absorption in the measurement plots.

4.3. Application of 3-PG$_{mix}$

3-PG$_{mix}$ can still be run as 3-PG$_{PJS}$ 2.7 and a comparison of predicted and observed biomass, volume, L and basal area was made for monospecific stands when using the light absorption model of 3-PG$_{PJS}$ 2.7 (L1) with the new light absorption model (L2, see Table 1 and Appendix A). For this comparison the 3-PG$_{PJS}$ 2.7 water balance calculations were used, but for all other simulations the new water balance calculations were used that account for vertical climatic gradients within the canopy of mixtures. The bias due to Jensen's Inequality was also calculated by providing the shape and scale parameters for Weibull B and w_s distributions.

3-PG is sensitive to the initial biomass inputs, especially with regards to initial canopy development (Sands and Landsberg, 2002). There was no information about the initial stand conditions, other than they were generally even aged and started with a total density of about 2500 trees per ha. Therefore, we assumed that the species proportions in terms of trees per ha that were measured during the inventory were the same as those when the stands established and that there was frequent (annual) and low intensity thinning until the final density that was observed during the inventory. All runs were initiated from age zero years with a seedling mass of 0.1 kg. More accurate predictions could probably be obtained by using known biomass inputs at a later age (e.g., Gonzalez-Benecke et al., 2014) but this information is much harder to obtain for mixtures than it is for monocultures, which are not subject to the effects of species interactions. Furthermore, initialising simulations from age zero forces 3-PG$_{mix}$ to reproduce all of the temporal stand dynamics as opposed to starting from known values at a later age. While starting at a later age should give more accurate predictions, it would not test the ability of 3-PG$_{mix}$ to reproduce all of the temporal dynamics.

4.4. Evaluation of model performance

The 3-PG$_{mix}$ output variables of stand volume, basal area, stem mass, leaf mass and the absorption of PAR were compared with the estimates from the plots. As explained above, the monospecific plots were used when calibrating the model and to determine the partitioning parameters and the plot fertility rating. Therefore, separate comparisons of observed and predicted values were made for monocultures and mixtures. The criteria used to make comparisons included the relative average error (average bias, e%, Eq. (1)), the relative mean absolute error (MAE%, Eq. (2)), and the mean square error (MSE, Eq. (3)) (Janssen and Heuberger, 1995; Vanclay and Skovsgaard, 1997).

$$e\% = 100\frac{\tilde{P} - \tilde{O}}{\tilde{O}} \quad (1)$$

$$\mathrm{MAE\%} = 100\frac{((\sum_n^{i=1}\left|P_i - O_i\right|)/n)}{\tilde{O}} \quad (2)$$

$$\mathrm{MSE} = \frac{\sum_n^{i=1}(P_i - O_i)^2}{n} \quad (3)$$

where, O are the observed values, P are the predicted values from 3-PG$_{mix}$, and $\tilde{O}$ and $\tilde{P}$ are the means. All statistical analyses were performed using R 3.0.2 (R Core Team, 2013).

A sensitivity analysis was carried out for parameters considered to be most important. Following Almeida et al. (2004a), the sensitivity analysis was based on changes to the parameters values of −20%, −10%, 10% and 20%.

4.5. Simulation of the spatial and temporal dynamics of species interactions

The 3-PG$_{mix}$ model was then used to simulate the effects of rainfall, soil fertility, stand density (thinning) and age on species interactions in mixed-species stands of *C. sclerophylla, C. lanceolata* and *L. formosana*, which were the most common species in the plots. The simulation was also used to test that the model predicted realistic temporal and spatial patterns similar to those that have been observed in the literature (Forrester, 2014a). A factorial design was used that included monocultures of each species and the three 2-species mixtures, three stand ages (where model predictions were compared; 10, 20 and 30 years), three stand densities (500, 1200 and 2000 trees per ha), five levels of soil fertility (FR = 0.5, 0.6, 0.7, 0.8, 0.9) and three levels of climate where long-term mean monthly precipitation of each month was multiplied by 0.67, 1 and 1.5. For all simulations the new light sub-model (L2) was used, within canopy climate conditions (E) were accounted for and bias was corrected.

The growth of a given species in mixture compared with its monoculture was examined by calculating a complementarity effect using Eq. (4) (Forrester, 2014a). The 0.5 accounts for the fact that the mixtures are 1:1 mixtures and the monocultures contain twice the number of trees per ha of a given species in mixture. A complementarity value of 1 indicates that the growth per tree of the given species was the same in mixture and monoculture. If it is >1 then the trees grew faster in mixture, and <1 indicates slower growth in mixtures.

$$\text{Complementarity} = \frac{\text{growth in mixture}}{\text{growth in monoculture} \times 0.5} \quad (4)$$

5. Results

Predicted and observed comparisons were made for monocultures using the light sub-model of 3-PG$_{PJS}$ 2.7 (L1) and the new light sub-model (L2) (Table 2). The comparisons were very similar and the new light model did not offer any significant improvement or result in any significant deterioration of predictions for these monospecific stands. Comparisons for mixtures could not be made because L1 cannot be used to predict the light absorption of mixtures.

The 3-PG$_{mix}$ model produced accurate predictions of stem mass (W_S) and basal area for monocultures with negligible bias (Table 2, Fig. 2). The foliage mass (W_F) predictions were slightly underestimated for stands with very high W_F, which had L of about 8–11. It is likely that these high "observed" values were overestimates and that the allometric equations used to estimate W_F and L should have accounted for stand density and not only stem diameter. However, the relatively small sample size of trees (68) used to establish the allometric equations was too small to find significant effects of stand density (Guisasola, 2014). The large range in values in Fig. 2 results largely from differences in stand density rather than age.

The model was also able to predict the W_S, W_F, L, volume and basal area of the each species in the mixtures (Fig. 2, Table 2). These predictions were not as accurate as those for the monocultures, which were used for calibration, but were always highly correlated with the observed values, with R^2 of at least 0.83. They also tended to underestimate the output variables, probably because the FR had been underestimated. The FR of mixed-species plots were taken from monospecific plots that were close to the mixtures, rather than actual soil characteristics of the mixed-species plots. The bias that was predicted to result from Jensens' inequality was generally less than 5% for each species in all 43 plots for B and w_s distributions and had a negligible effect on the predicted outputs (data not shown).

The canopy structure of these native forests was very variable in terms of stand density, species composition and vertical structure. Despite this, the light sub-model within 3-PG$_{mix}$ provided predictions of species-specific light absorption that were highly correlated with predictions from the much more detailed 3D tree-level model Maestra (Fig. 3).

Table 2
Statistical information that describes the relationships between the predicted and observed variables for mixtures (bold font) or monocultures (plain font) using different sub-models; L1 = 3-PG$_{PJS}$ 2.7 light sub-model, L2 = new light sub-model, E = evapotranspiration calculations that account for within-canopy VPD, net radiation and g_a. Output variables include foliage mass (W_F), stem mass (W_S), stand volume (V), leaf area index (L) and basal area (BA). The statistical information includes the relative average error (e%), the relative mean absolute error (MAE%) and the mean square error (MSE).

Sub-models used	Variable	e%	MAE%	RMSE	R^2
L2, E	W_S	−3.4	11.4	248.1	0.99
L2, E	W_F	−7.7	19.8	4.5	0.96
L2, E	L	−5.7	19.8	1.4	0.95
L2, E	V	−12.5	16.5	1114.9	0.98
L2, E	BA	−1.9	9.2	10.1	0.99
L2, E	**W_S**	**−20.2**	**28.8**	**940.6**	**0.94**
L2, E	**W_F**	**−0.4**	**25.7**	**2.1**	**0.93**
L2, E	***L***	**−19.3**	**34.1**	**3.7**	**0.84**
L2, E	**V**	**−26.2**	**32.1**	**1942.3**	**0.94**
L2, E	**BA**	**−16.9**	**24.8**	**31.6**	**0.95**
L2	W_S	−0.3	10.9	225.1	0.99
L2	W_F	−4.9	18.8	4.0	0.96
L2	L	−2.8	19.4	1.3	0.95
L2	V	−9.6	14.6	887.0	0.98
L2	BA	0.5	8.8	9.3	0.99
L1	W_S	13.8	16.0	610.8	0.99
L1	W_F	12.8	19.6	3.7	0.96
L1	L	14.8	20.8	1.2	0.96
L1	V	5.0	12.6	635.4	0.99
L1	BA	12.3	13.6	23.6	0.99

The model sensitivity to the parameters was similar but not identical for each species. To summarise these effects Table 3 shows how much these output variables changed in relation to the change in the parameters. The parameters to which outputs of at least one species were highly sensitive included p_{20}, k_H, α_{Cx}, σ_1. The output variable that was most affected by changes in the parameters was W_F. Of the parameters tested, those that had the smallest effect on the outputs were the maximum litterfall rate (γ_{Fx}) and the parameter that describes the stomatal response to VPD (k_D).

The results of the simulation experiment suggested that *L. formosana* and *C. sclerophylla* were more competitive than *C. lanceolata* during the first decade and there was generally a positive complementarity effect on their NPP when they were growing in mixtures with *C. lanceolata* (Fig. 4). In turn, the predicted NPP of *C. lanceolata* was generally lower in mixture than in its monoculture (Fig. 4). These differences declined with time as the *C. lanceolata* overtopped the broad-leaved species (Fig. 5). There was very little temporal change in the complementarity effect predicted for *C. sclerophylla*, and there was only a temporal change (a decline) in complementarity predicted for *L. formosana* when it lost its dominance against *C. lanceolata*.

The simulations suggest that *L. formosana* benefited from being in mixtures more when fertility was low or when stand density was high. In contrast, when mixed with *L. formosana*, each of the other species were predicted to experience increasing complementarity effects as fertility increased, or decreasing complementarity as density increased. A moderate increase in complementarity was also predicted for *C. sclerophylla* as fertility increased when mixed with *C. lanceolata*, but *C. lanceolata* did not show a corresponding decrease. The interactions between species and their responses to stand density show that 3-PG$_{mix}$ could potentially be used to develop silvicultural regimes for mixed and monospecific stands (Fig. 6).

These simulated complementary effects were related to competition for light and the complementary pattern for the absorption

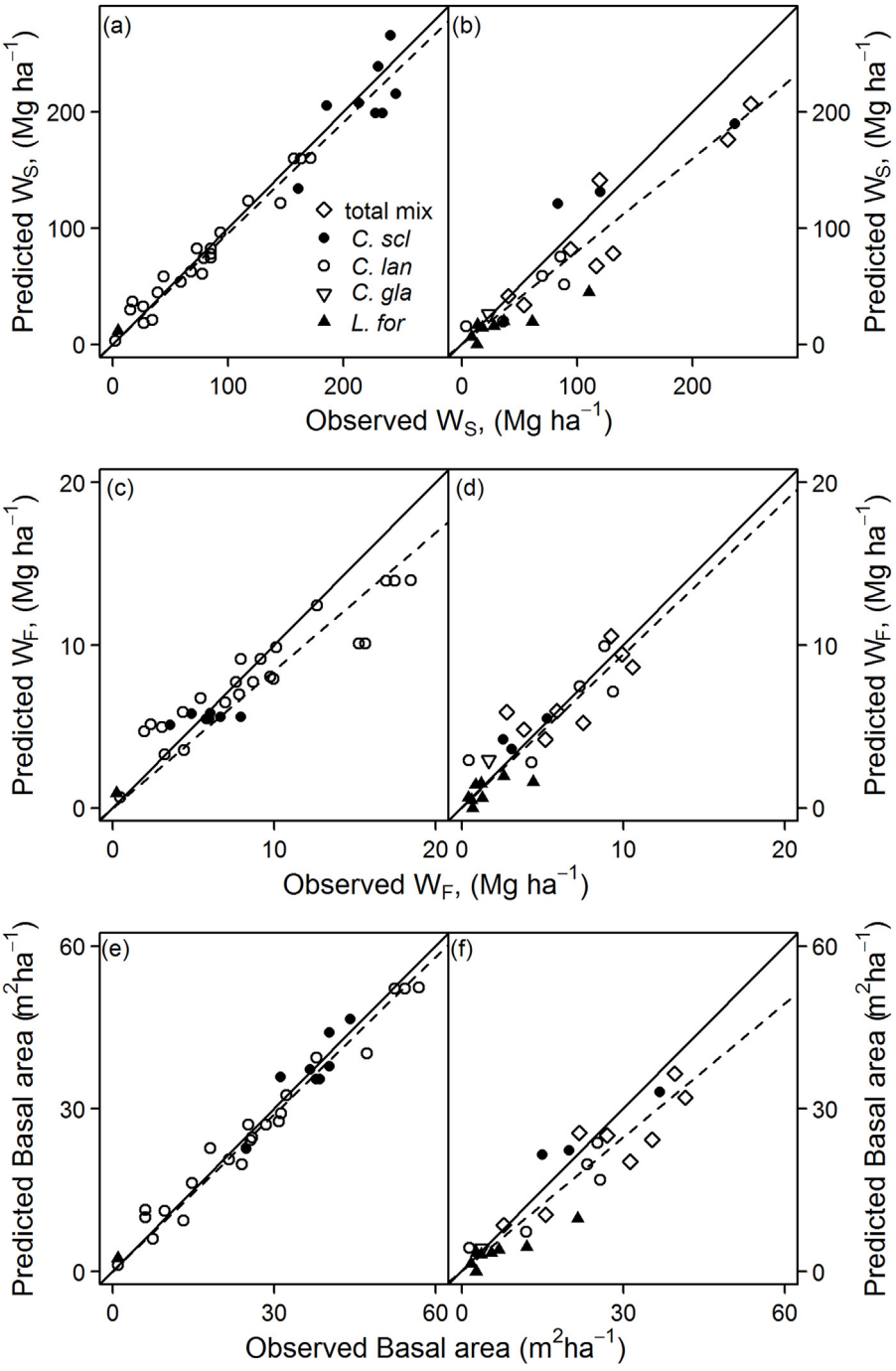

Fig. 2. Comparison of observed (in the 2013 inventory) and predicted stand stem mass (W_S, a,b), foliage mass (W_F, c,d), and basal area (e,f) for monocultures (a,c,e) and mixed-species stands (b,d,f) of *C. sclerophylla* (*C. scl*), *C. lanceolata* (*C. lan*), *C. glauca* (*C. gla*) and *L. formosana* (*L. for*). The "total mix" is the sum for all species within the mixture. The solid lines are 1:1 lines and the dashed lines are lines fitted to the data that pass through the origin.

of PAR (ϕ_{pa}) was the same as that for NPP. The light-use efficiency (NPP per ϕ_{pa}) of a given species did not change when it was in a mixture because the growth modifiers had similar effects in all stands under the same level of a given factor. The VPD and soil water availability had minor effects and their modifiers were a minimum of 0.78 in all treatments.

6. Discussion

The stands used for this study included a wide range of stand structures, in terms of stand density, species composition and species proportions as well as soil fertility. The 3-PG$_{mix}$ model was able to predict the growth, biomass partitioning and light absorption of the individual species within these mixed-species forests. The simulations also indicated that the interactions between these species (and complementarity effects) varied with stand age, stand density, fertility and rainfall. The 3-PG$_{mix}$ model therefore has the potential to be a management tool for mixed-species forests as well as monocultures, and also to examine the effects of changing stand density by thinning or other disturbances.

A thorough evaluation of a process-based model should include an assessment of all of the processes that the model includes

Table 3
Results of the sensitivity analysis of changes in the values of the parameters of foliage to stem partitioning ratios for B of 2 and 20 cm (p_2, p_{20}), the stem allometric exponent (n_S), the maximum and minimum fraction of NPP allocated to roots (η_{Rx}, η_{Rn}), the maximum litterfall rate (γ_{Fx}), the light extinction coefficient (k_H), canopy quantum efficiency (α_{Cx}), the stomatal response to VPD (k_D), the maximum canopy conductance (g_{Cmax}), the L required for g_{Cmax} (L_{gCmax}) and the specific leaf area of older stands (σ_1) on the output variables of foliage mass (W_F), root mass (W_R), stem mass (W_S), volume (V), volume mean annual increment (MAI), L, B, height (h), and whole rotation absorbed PAR (ϕ_{paR}), NPP, transpiration (Tr), rainfall interception (RI) and evapotranspiration (ET).

Parameter	*Castanopsis sclerophylla*	*Cunninghamia lanceolata*	*Liquidambar formosana*
High sensitivity (Δ% in output ≥ Δ% in parameter)			
p_{20}		W_F, L	L
k_H		W_F, V, MAI, h, ϕ_{paR}	
α_{Cx}	W_F, W_R, W_S, V, MAI, L, NPP, Tr, RI, ET	W_F, W_R, W_S, V, MAI, L, NPP, RI, ET	W_F, W_R, W_S, V, MAI, L, NPP, Tr, RI, ET
σ_1	L, RI	V	L
Medium sensitivity (Δ% in output ≥ 0.5 × Δ% in parameter)			
p_{20}	W_F, L	W_F, L	
n_S	W_F, L	W_F, L	W_F, L
η_{Rn}	W_R	W_R	W_R
k_H	W_S, V, MAI, ϕ_{paR}, RI	W_F, W_R, W_S, V, MAI, L, ϕ_{paR}, NPP, RI	
α_{Cx}	W_F, W_R, W_S, V, MAI, L, B, ϕ_{paR}, NPP, Tr, RI, ET	W_F, W_R, W_S, V, MAI, L, B, ϕ_{paR}, NPP, RI, ET	W_F, W_R, W_S, V, MAI, L, B, ϕ_{paR}, NPP, Tr, RI, ET
g_{Cmax}	Tr	Tr	Tr
σ_1	L, Tr, RI, ET	W_F, W_R, W_S, V, MAI, L, ϕ_{paR}, NPP, RI	L, RI
Low sensitivity (Δ% in output ≥ 0.25 × Δ% in parameter)			
p_2	Tr, RI	WS, V, MAI, ϕ_{paR}, NPP, Tr, RI, ET	W_F, L, RI
p_{20}	W_F, L, RI	W_F, W_R, L	W_F, L, RI
n_S	W_F, L, RI	W_F, W_R, L, ϕ_{paR}, NPP	W_F, L
η_{Rx}	W_R		W_R
η_{Rn}	W_R	W_R	W_R
k_H	W_F, W_R, W_S, V, MAI, L, ϕ_{paR}, NPP, Tr, RI, ET	All output variables	W_F, W_S, V, MAI, ϕ_{paR}, NPP, Tr, RI
α_{Cx}	All output variables	All output variables	All output variables
g_{Cmax}	Tr, ET	Tr, ET	Tr, ET
L_{gCmax}	W_F, L		
σ_1	L, ϕ_{paR}, Tr, RI, ET	W_F, W_R, W_S, V, MAI, L, ϕ_{paR}, NPP, RI, ET	L, Tr, RI, ET
Very low sensitivity (Δ% in output < 0.25 × Δ% in parameter)			
γ_{Fx}, k_D,	All output variables		

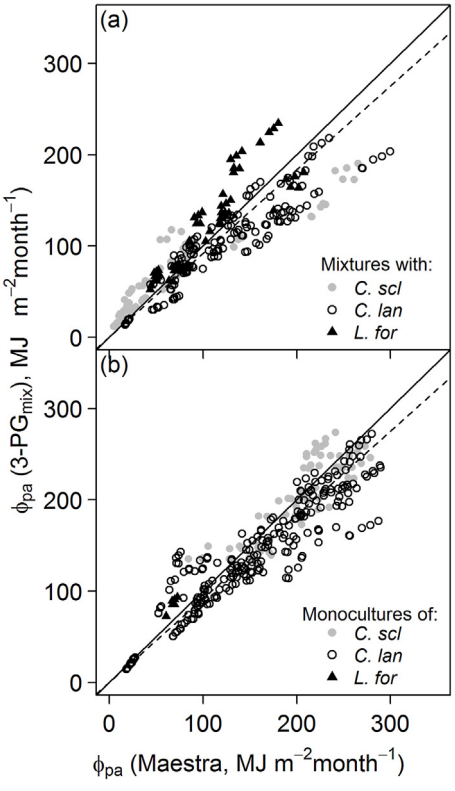

Fig. 3. Comparison of the predicted absorption of photosynthetically active radiation ϕ_{pa} from the Maestra model and predictions from 3-PG$_{mix}$ in mixed-species (a) or monospecific stands (b) of *C. sclerophylla* (*C. scl*), *C. lanceolata* (*C. lan*) and *L. formosana* (*L. for*). The solid lines are 1:1 lines and the dashed lines are lines fitted to the data that pass through the origin.

(Grimm, 1999; Weiskittel et al., 2010) because it is easy to get a very good fit to observed growth data for the wrong physiological reasons (Sands, 2004a). All of the processes considered by 3-PG have been compared with empirical data (Landsberg and Sands, 2010), including those examined in this study and others such as biomass partitioning (Landsberg et al., 2005; Gonzalez-Benecke et al., 2014; González-García et al., in press), litterfall (Zhao et al., 2009), the water balance (Dye, 2001; Almeida et al., 2004a, 2007, 2010; Feikema et al., 2010b; Wei et al., 2014a; González-García et al., in press; Almeida and Sands, 2015), responses to CO_2 (Almeida et al., 2009), diameter distributions (Landsberg et al., 2005), density-dependent and density-independent mortality (Sands and Landsberg, 2002; Gonzalez-Benecke et al., 2014; González-García et al., in press) and $\delta^{13}C$ of wood (Wei et al., 2014a,b). Such detailed evaluations are not often done for process-based models, including those that have actually been used for mixed-species forests (Pretzsch et al., 2015), which reduces confidence (Sands and Landsberg, 2002) that such models are capable of predicting realistic complementarity effects.

The predicted-observed comparisons for 3-PG described above are probably also applicable to 3-PG$_{mix}$. The main change to 3-PG$_{mix}$ was the new light sub-model. Predictions for monocultures differed very little between 3-PG$_{PJS}$ 2.7 and 3-PG$_{mix}$ when each used a different light sub-model (L1 vs. L2; Table 2). Furthermore the sensitivity analysis indicated similar model behaviour to previous sensitivity analyses of 3-PG in terms of the parameters that 3-PG is most sensitive too and the output variables that are most sensitive to them (Almeida et al., 2004a; Esprey et al., 2004; Xenakis et al., 2008; Zhao et al., 2009; Pérez-Cruzado et al., 2011; Potithep and Yasuoka, 2011).

Confirming that all component processes are predicted correctly is particularly important when modelling mixed-species or uneven-aged forests because each species (or cohort) can influence the others and cause feedback effects on the longer-term stand dynamics. It is critical to check that no species is being given an

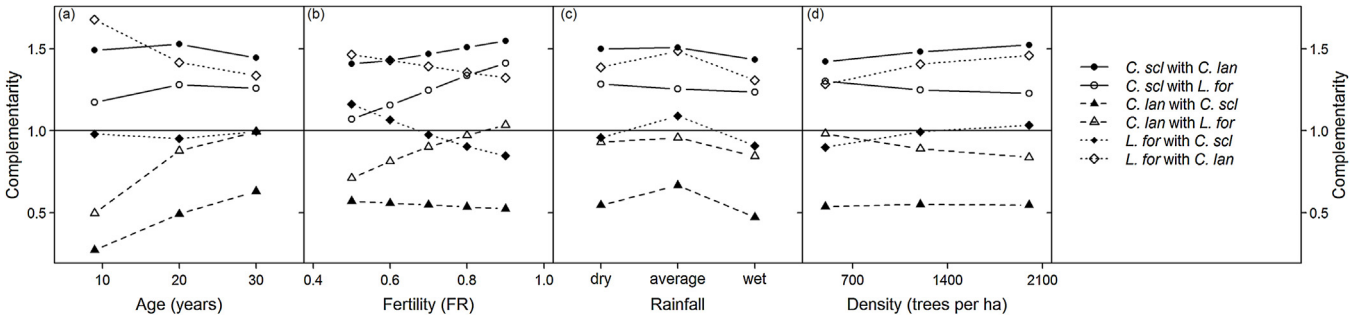

Fig. 4. The simulated complementarity effect (calculated using NPP and Eq. (4)) for each species in the mixed-species stands containing *C. sclerophylla* (*C. scl*), *C. lanceolata* (*C. lan*) and *L. formosana* (*L. for*) along the age, fertility, rainfall and stand density gradients described in the text. If complementarity is >1 then trees of the given species grew faster in mixture than monoculture, whereas if complementarity is <1 then trees of the given species grew slower in the mixture than its monoculture.

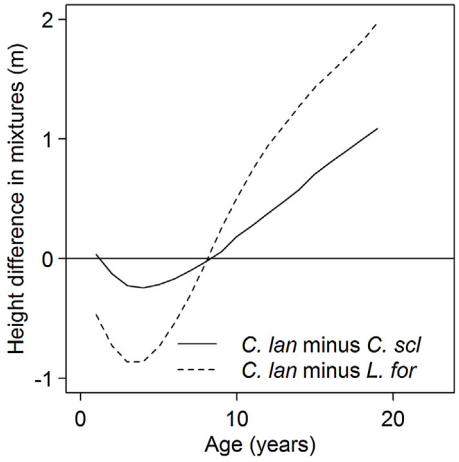

Fig. 5. The simulated difference in height of *C. lanceolata* (*C. lan*) and either *C. sclerophylla* (*C. scl*) or *L. formosana* (*L. for*) when growing in 1:1 mixtures containing a total of 2000 trees per ha, with the mean climate and a fertility rating of 0.7 for each species.

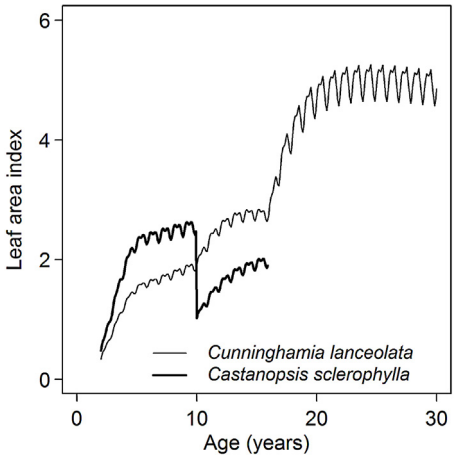

Fig. 6. An example of the use of 3-PG$_{mix}$ to examine how two species interact in a mixture and respond to thinning. *Cunninghamia lanceolata* and *Castanopsis sclerophylla* are planted in a 1:1 mixture (500 trees per ha each) and *C. sclerophylla* is thinned to 200 trees per ha at age 10 years and zero trees per ha at age 15 years. The wavy pattern of each line reflects the seasonality of leaf production.

unrealistic competitive advantage or disadvantage. For example, some models predict light absorption by assuming that all of the foliage of a given cohort is at the top of the crown (Bugmann, 2001). This is no problem when there is no vertical overlap between the cohorts (Fig. 1d), but this is often not the case in mixed-species forests and can result in an overestimation of light absorption by taller species and an underestimate for shorter species (Forrester et al., 2014), which would lead to unrealistic stand dynamics and species interactions. Similarly, it may also be important to correct for bias resulting from Jensen's Inequality due to the use of allometric equations within 3-PG$_{mix}$ because this could potentially lead to unrealistic competitive advantages in terms of height or crown sizes. This bias can be accounted for in 3-PG$_{mix}$ when necessary but in this study the bias was usually less than 5%.

The calibration of 3-PG$_{mix}$ was based on data from monocultures and then 3-PG$_{mix}$ was applied to mixed-species plots in the same stand. An independent validation should use different stands to validate the model. It would also be preferable to have a more carefully designed experimental data set. The simplest case could be a two-species mixture as well as monocultures of both species at the same site. This "triplet" could then be replicated at many different sites that vary in soil and climatic conditions, or by applying fertiliser application, irrigation and thinning treatments at a single site. Such a design would enable comparisons of observed and predicted complementarity effects on each species and the spatial and temporal dynamics of these complementarity effects (using Eq. (4)), as opposed to simply comparing biomass, or light absorption as in Figs. 2 and 3. These spatial and temporal dynamics of complementarity effects could be expected to be consistent with those found in a review of measured patterns in mixed-species forests (Forrester, 2014a). The triplet design is similar to the "twin plot" approach used to examine fertiliser responses at 127 locations in *Eucalyptus* plantations in Brazil (Stape et al., 2006). A similar approach could be used to compare observed and predicted thinning responses.

Several studies have shown that 3-PG can predict thinning responses or the effects of stand density (Rodríguez et al., 2002; Landsberg et al., 2005; Miehle et al., 2009; Gonzalez-Benecke et al., 2014; López-Serrano et al., 2015) but it has also been noted that 3-PG may not accurately predict these responses in some stands (Sands, 2004b; Pérez-Cruzado et al., 2011). This is because increased biomass partitioning to foliage as opposed to stems can result from reductions in stand density (Bernardo et al., 1998; Forrester et al., 2012) but this is not directly accounted for in 3-PG. Another reason is that the original light sub-model (L1) may provide biased predictions of light absorption for canopies that are opened by thinning (Landsberg and Sands, 2010). The light predictions in 3-PG$_{mix}$ (L2) can account for the opening of canopies after thinning and have been tested for a range of stand densities and for different species (Forrester et al., 2014). Also, the allometric

equations used to predict stem (or foliage) mass from tree diameter in this study were not influenced by stand basal area, possibly because the stands were subject to frequent and low intensity thinning that prevented these effects from developing (Guisasola et al., 2015). While 3-PG predictions following thinning have been tested in terms of growth, diameter distributions (Rodríguez et al., 2002; Landsberg et al., 2005; Miehle et al., 2009; López-Serrano et al., 2015) and light (this study), thinning responses in terms of other processes, such as transpiration have not yet been tested.

In contrast to light and water, 3-PG includes a relatively crude procedure to quantify nutrition. Soil and nutritional limitations tend to be the most difficult components to include in process-based models (Johnsen et al., 2001). Based on current knowledge, it is infeasible to model nutrient availability, nutrient uptake and associated species interactions, while at the same time maintaining 3-PG as a simple and generally applicable model (Landsberg et al., 2005). The disadvantage of this is when nutrient-related species interactions such as symbiotic nitrogen fixation or accelerated rates of nutrient cycling (Richards et al., 2010) are considered to be important. This could be modelled empirically in 3-PG$_{mix}$ by changing the *FR* for a given species as the stand develops. Alternatively, 3-PG$_{mix}$ could be coupled with models dealing with nutrient cycling (Landsberg and Sands, 2010) and the choice of model could depend on the nutrients considered to be most important in the region and the nutrients that are influenced by the species within the mixture. For example 3-PG has previously been coupled to the soil organic matter decomposition model ICBM/2N (Andrén and Kätterer, 1997) to include several soil carbon and nitrogen pools (Xenakis et al., 2008).

The simulation shown in Fig. 4 is an example of how 3-PG$_{mix}$ might be used to develop silvicultural regimes for mixed-species stands on different sites. The species interactions changed as the stands developed, across gradients in fertility and rainfall and also at different stand densities. Such predictions could be used to determine potential species compositions, species proportions and thinning regimes for new plantations or the responses of existing mixtures to modifications in species proportions, stand density and climate. It would also indicate the fertility and climatic conditions that are most likely to be appropriate for certain species combinations and thereby help to avoid the establishment or management of mixtures where they may be more susceptible than monocultures or other mixtures to factors such as drought stress. The model could also show some of the main processes or interactions that lead to the spatial and temporal dynamics, for example in terms of water and light use, or use efficiencies. It is clear that these simulations will not replace empirical data but they could provide early indications while waiting for the results of long-term experiments. Models for mixed-species stands that cannot reproduce these spatial and temporal dynamics might as well be simplified by modelling monocultures and predicting the growth of mixtures using the weighted averages of the monocultures.

Acknowledgements

This study was part of a Sino-German Cooperation on Innovative Technologies and Service Capacities of Multifunctional Forest Management project (Lin^{2}Value, projec number 033L049-CAFYBB2012013) supported by the Federal Ministry of Education and Research (BMBF) and Chinese Academy of Forestry. We thank Dr. Lutz Fehrmann, Prof. Christoph Kleinn, Prof. Christian Ammer, Dr. Hans Fuchs, Sabine Schreiner, Dr. Haijun Yang, Dr. Torsten Vor, Rubén Guisasola and Dengkui Mo for assistance with the plot design and fieldwork for the inventory. We also thank Director An'guo Fan, Mr. Bailing Ding and Ms Yue'e Chu from the Shitai Forest bureau for their assistance when organising fieldwork. Thanks also to Mr Xiaozhu Wang and Mr Hongbing Ruan for fieldwork support. Lastly, we would like to thank Prof. Jürgen Bauhus, Matthias Seebauer, Dr. Auro Almeida, Dr. Peter Sands, Dr. Liang Wei, Dr. Joe Landsberg, Dr. Dick Waring and two anonymous reviewers for their useful comments during this project and on the manuscript.

Appendix A. Summary of the equations used by 3-PG$_{mix}$

The values and units of the parameters used for the species in this study are shown in Table 1.

A.1. Gross and net primary production

A major underlying principle of 3-PG is the linear relationship between production and the absorption of photosynthetically active radiation (ϕ_{pa}). Often production refers to above-ground biomass and the slope of this relationship is the light-use efficiency (ε). In 3-PG, calculations start with production as gross primary production (GPP or P_G) and the slope of the relationship between P_G and ϕ_{pa} is the canopy quantum efficiency α_C.

$$P_G = \alpha_C \phi_{pa} \tag{A.1}$$

The α_C is calculated from the species-specific maximum potential α_C (α_{Cx}) and several dimensionless growth modifiers that take values between 0 for extremely limiting conditions and 1 for optimal conditions (Landsberg and Waring, 1997; Sands and Landsberg, 2002). The modifiers account for the effects of temperature (f_T), frost (f_F), atmospheric vapour pressure deficit (VPD) (f_D), available soil water (f_θ), soil nutrition (f_N), atmospheric CO_2 (f_C) and stand age (f_{AGE}), such that

$$\alpha_C = \alpha_{Cx} \varphi f_T f_F f_N f_C \tag{A.2}$$

The φ is a physiological modifier (PhysMod) that can be calculated using either the most limiting of soil water and VPD (Eq. (A.3a); the original form used in 3-PG), or allows both soil water and VPD to have an effect, based on Jarvis (1976), and also used in Wei et al. (2014a) and Feikema et al. (2010b) (Eq. (A.3b)). PhysMod is used when predicting gross primary production (Eq. (A.4)), canopy conductance (Eq. (A.40)–(A.41)) and partitioning to roots (Eq. (A.26)).

$$\varphi = f_{AGE} \min\left\{f_D, f_\theta\right\} \tag{A.3a}$$

$$\varphi = f_{AGE} f_D f_\theta \tag{A.3b}$$

Then from Eqs. (A.1)–(A.3)

$$P_G = f_T f_F f_N f_C \varphi \alpha_{Cx} \phi_{pa} \tag{A.4}$$

The default ratio (Y) to convert P_G to net primary production (NPP) is 0.47.

A.2. Growth modifiers

The temperature modifier is given by

$$f_T(T_a) = \left(\frac{T_a - T_{min}}{T_{opt} - T_{min}}\right)\left(\frac{T_{max} - T_a}{T_{max} - T_{opt}}\right)^{(T_{max}-T_{opt})/(T_{opt}-T_{min})} \tag{A.5}$$

where, $f_T \geq 0$ and $f_T = 0$ if $T_a > T_{max}$ or $T_a < T_{min}$ (Sands and Landsberg, 2002). T_a is the mean monthly temperature and T_{min}, T_{opt} and T_{max} are the minimum, optimal and maximum temperatures for growth.

A temperature modifier (f_{gT}) of the same form as f_T can be applied when calculating canopy conductance (g_c, Eqs. (A.40) and (A.41)) (Feikema et al., 2010b). This is calculated using the daytime mean temperature rather than T_a. The daytime mean temperature is estimated as the mean of T_{max} and T_a (not T_{min}) (Feikema et al., 2010b).

The frost modifier is

$$f_F(d_f) = 1 - k_F\left(d_f/30\right) \quad (A.6)$$

where, d_f is the mean number of frost days per month and k_F is the number of days of production lost for each frost day (Landsberg and Waring, 1997).

The nutrition modifier is given by

$$f_N(FR) = 1 - (1 - f_{N0})(1 - FR)^{n_{fN}} \quad (A.7)$$

where, FR is the fertility rating, f_{N0} is the value of f_N when FR = 0, and n_{fN} is a power (Almeida et al., 2004a). FR can be between 0 (very limited nutrition) and 1 (non-limiting nutrition). The FR is species specific so different species within a given mixture could have different FR at the same site. Facilitative inter-specific interactions in mixed-species stands that change nutrition (e.g. symbiotic N_2 fixation, nutrient cycling) can be examined by empirically changing the FR of any given species that experiences a change (increase or decrease) in nutrition as a stand develops. This FR effect is not designed to account for changes in nutrient availability that result from competitive exclusion where nutrient uptake for one species might increase simply because the other is a poorer competitor. That case is already taken into account because species that grow larger reduce the light absorption, growth and water use of smaller species and use more nutrients.

Vapour pressure deficit can reduce growth by directly influencing stomatal and canopy conductance; increasing VPD reduces conductance for many species. The vapour pressure deficit modifier is defined as

$$f_D(D) = e^{-k_D D} \quad (A.8)$$

where, D is mean daytime VPD and k_D defines the stomatal response to VPD (Landsberg and Waring, 1997). The soil water modifier is defined as

$$f_\theta\left(\theta_S\right) = \frac{1}{1 + \left[\left(1 - \theta_S/\theta_{Sx}\right)/c_\theta\right]^{n_\theta}} \quad (A.9)$$

where, θ_S is the available soil water, θ_{Sx} is the maximum available soil water, and n_θ and c_θ reflect differences in the relationship between transpiration rate and soil water content for different soil textures (Landsberg and Waring, 1997).

Declines in current annual increment of forests after a peak close to the time of maximum L have been observed for many species (Ryan et al., 1997) and this decline is given by an empirical age modifier as

$$f_{AGE}(t) = \frac{1}{1 + \left[\left(t/t_x\right)/r_{age}\right]^{n_{age}}} \quad (A.10)$$

where, t_x is the maximum stand age, r_{age} is the relative age to give the $f_{AGE} = 0.5$ and n_{age} is the power (Landsberg and Waring, 1997). This modifier is often disabled, as in this study (r_{age} and n_{age} result in $f_{AGE} = 1$), especially when the modelled stands are not close to their maximum potential height.

The CO_2 modifier is defined differently depending on whether it is applied when calculating canopy conductance g_c (f_{Cg}) or P_G ($f_{C\alpha}$) (Almeida et al., 2009; Landsberg and Sands, 2010).

$$f_{C\alpha}(CO_2) = f_{C\alpha x} \times \frac{CO_2}{350 \times (f_{C\alpha x} - 1) + CO_2} \quad (A.11)$$

$$f_{Cg}(CO_2) = \frac{f_{Cg0}}{1 + \left(f_{Cg0} - 1\right) \times CO_2/350} \quad (A.12)$$

Where

$$f_{C\alpha x} = \frac{f_{C\alpha 700}}{2 - f_{C\alpha 700}} \quad (A.13)$$

$$f_{Cg0} = \frac{f_{Cg700}}{2 \times f_{Cg700} - 1} \quad (A.14)$$

The CO_2 is the atmospheric CO_2 (ppm) at the site and does not vary during a simulation, as opposed to the (optional) c_a used in Eq. (A.46), which is monthly atmospheric CO_2 (ppm) and when provided it will be used instead of the constant site CO_2. The α_{C700} and g_{C700} parameters define the species-specific responses to changes in atmospheric CO_2.

A.3. Light absorption

There are two options to calculate ϕ_{pa}, both of which are based on the Lambert-Beer Law, such that the fraction of photosynthetically active radiation (ϕ_p) that is absorbed by the canopy, f (i.e. ϕ_{pai}/ϕ_p) is given by

$$f = 1 - e^{-kL} \quad (A.15)$$

where, k is a light extinction coefficient and L is the leaf area index ($m^2\,m^{-2}$). The first approach to predict ϕ_{pa} (option L1 in Table 1) is following the method used in 3-PG$_{PJS}$2.7 that was modified by Sands (2004a) where ϕ_{pa} is determined from total incoming solar radiation and L as

$$\phi_{pa} = \left(1 - e^{-kL/\zeta}\right) 2.3\zeta\bar{Q}\Delta t \quad (A.16)$$

where, ζ is the proportion of ground area covered by the canopy and $\bar{Q}$ ($MJ\,m^{-2}\,d^{-1}$) is the mean daily solar radiation above the canopy over the time period Δt (Sands, 2004a). The factor of 2.3 converts total radiation into ϕ_p ($2.3\,mol\,MJ^{-1}$). The ζ is calculated as a function of age, such that it is 1 after the canopy closes and prior to canopy closure it is the ratio of age/age of canopy closure (Eqs. (A.30) and (A.31)). ζ is therefore not influenced by thinning.

$$L = 0.1\sigma W_F \quad (A.17)$$

where, σ (m^2/kg) is specific leaf area (SLA) and the 0.1 converts $Mg\,ha^{-1}$ to $kg\,m^{-2}$ (Landsberg and Waring, 1997). SLA declines with age such that

$$\sigma(t) = \sigma_1 + (\sigma_0 - \sigma_1)\, e^{-(\ln 2)(t/t_\sigma)^2} \quad (A.18)$$

where, σ_0 and σ_1 are the values of σ in young and older stands, respectively, and t_σ is the age at which $\sigma = ½(\sigma_0 + \sigma_1)$ (Sands and Landsberg, 2002).

The use of Eq. (A.16) to calculate ϕ_{pa} is appropriate for monospecific stands with horizontally and vertically uniform canopies. However, even in those stands the extinction coefficient (k) can vary, for a given species, with age, season and site quality (Cannell et al., 1987; Binkley et al., 2013), so care must be taken using this approach because it can result in biased predictions of ϕ_{pa} (see Fig. 5b in Forrester et al., 2014). Part of the bias due to horizontal canopy heterogeneity (e.g. open canopies) can be accounted for by the ζ term in Eq. (A.16), but this is only used before the canopy closes and therefore not after thinning, although Gonzalez-Benecke et al. (2014) calculated it using allometric relationships between tree diameter and crown projection area. Furthermore, when canopies are not closed there are two mechanisms that need to be accounted for. One is the reduction in ground area covered by the canopy (i.e. ζ), and another is the fact that individual tree ϕ_{pa} (for a given crown size) will be higher in an open than in a closed canopy stand because there is less shading by neighbouring trees. The ζ term in Eq. (A.16) may not adequately account for this (Forrester et al., 2014). This is important in stands that do not have closed canopies, such as young forests, thinned forests or naturally disturbed forests. Furthermore, Eq. (A.16) will not work for mixed-species forests, except for the special case where each species forms a distinct canopy layer (with no vertical overlap between layers)

and preferably when each canopy layer is closed, which is usually not the case for the lower layers. However, it is critical to note that even with this special case of canopy stratification, L1 cannot be used for mixtures because it has only been programmed for monocultures and ignores competition for light from any competing species.

Therefore, ϕ_{pa} can also be predicted using a second approach (option L2 in Table 1) that can account for vertically and horizontally heterogeneous canopies e.g., thinned stands, mixed-species stands or uneven-aged stands where there is vertical overlap between the crowns of different cohorts or species, and/or horizontal variability in leaf area due to the mixing of cohorts or species, and gaps in the canopy resulting from disturbances (Forrester, 2014b; Forrester et al., 2014). For this approach ϕ_{pa} for the ith species in the jth (vertical) canopy layer ($\phi_{pa_{ij}}$) is predicted using Eq. (A.19) (Forrester et al., 2014).

$$\emptyset_{pa_{ij}} = \lambda_{v_i}\lambda_{h_j}\left[1 - e^{\left(-\sum_{i=1}^{n} k_{H,i}L_i\right)}\right] 2.3\bar{Q}\Delta t \quad (A.19)$$

The k_H is defined as an extinction coefficient for a homogeneous canopy (Duursma and Mäkelä, 2007). This is required because typical long-term (monthly, annual) extinction coefficients, k (Eqs. (A.15) and (A.16)) vary for a given species when the crown architecture and canopy structures change (Binkley et al., 2013). A homogeneous canopy is defined as one composed of trees of the same height, with the same live-crown length, having box-shaped crowns that fit together perfectly (no space between crowns), and of the same leaf-area density (LAD, leaf area per crown volume, $m^2\,m^{-3}$), leaf angle distribution, leaf reflectance and leaf transmittance. k_H is therefore independent of trees per ha.

The λ_{v_i} is an empirical parameter that partitions the ϕ_{pa} to each of the i species within a given layer (j) based on the vertical structure (relative species heights) of the layer as well as the k_H and L of each species (Eq. (A.20)).

$$\lambda_{v_i} = 0.0123 + 0.2366\frac{k_{H,i}L_i}{\sum_n^{i=1} k_{H,i}L_i} + 0.0291\frac{h_{m,i}}{h_m} + 0.6084\frac{k_{H,i}L_i}{\sum_n^{i=1} k_{H,i}L_i}\frac{h_{m,i}}{h_m} \quad (A.20)$$

The $h_{m,i}$ is the mid-crown height of species i and h_m is the mid-crown height of the layer in which species i belongs (Forrester et al., 2014). The mid-crown-height is the height of a point half way between tree height and the height to crown base (H_b), where the H_b is the height where the lowest live branch joins the stem. Thus, the mid-crown height of a given species is calculated as (height−H_b)/2 + H_b; the mid-crown height of a given layer is calculated using the height of the tallest species in that layer, and the minimum H_b of all species in that layer. Eq. (A.20) has been tested for a wide range of crown architectures, species, species combinations, stand densities and vertical stand structures (Forrester, 2014b; Forrester et al., 2014).

The horizontal heterogeneity λ_{h_j} is a function of mean midday solar zenith angle, k_H, the ratio of mean tree leaf area (L_A) to mean tree crown surface area (S_A) and v_{frac}, which is the sum of the crown volume (m^3) of all crowns within a given layer within one hectare divided by the total volume of that layer (m^3) (Eqs. (A.21) and (A.22); Forrester et al., 2014). The total volume of a layer is (height of the tallest species−minimum H_b) × 100 m × 100 m. The v_{frac} quantifies canopy openness and therefore the potential inter-tree shading, which increases as the mean midday zenith angle increases due to season and latitude. The zenith angle used to calculate λ_{h_j} is an adjusted value, z_{adj}. This is needed because mean midday solar zenith angle is a sine-shaped function of Julian day, but at latitudes of <23°, the sine shape is distorted when solar zenith angles decline to 0 and increase again, instead of continuing to decline below zero, which would maintain the sine shape (see Appendix B in Forrester et al., 2014). The z_{adj} allows that part of the curve to be negative (× −1). The λ_{h_j} is then calculated using two empirical Eqs. (A.21) and (A.22) because z_{adj} does not influence λ_{h_j} until it is greater than 30°. These are general equations that can be applied to any species and stand structure.

$$\lambda_{h_j, z_{adj}\le 30} = 0.8260 + \left(1.1698 - 0.9221\,k_H\frac{L_A}{S_A}\right) \times 0.1^{v_{frac}} - 0.6703 \times 0.1^{v_{frac}} \quad (A.21)$$

$$\lambda_{h_j, z_{adj}>30} = 0.8260 + 0.0011 \times 1.0807^{z_{adj}} + \left(1.1698 - 0.9221\,k_H\frac{L_A}{S_A}\right) \times 0.1^{v_{frac}} - 0.6703 \times 0.1^{v_{frac}} \quad (A.22)$$

A.4. Biomass pools and partitioning

The NPP is divided into foliage (W_F), root (W_R) and stem biomass (W_S) based on McMurtrie and Wolf (1983)

$$\Delta W_F = \eta_F P_n - \gamma_F W_F \Delta t - m_F\left(W_F/N\right)\Delta N \quad (A.23)$$

$$\Delta W_R = \eta_R P_n - \gamma_R W_R \Delta t - m_R\left(W_R/N\right)\Delta N \quad (A.24)$$

$$\Delta W_S = \eta_S P_n - m_S\left(W_S/N\right)\Delta N \quad (A.25)$$

where, ΔW_i is the change in the ith pool over a time interval of Δt days, η_i is the fraction of NPP partitioned to the ith pool, γ_F (days^{-1}) is the litterfall rate, γ_R (days^{-1}) is the root turnover rate, N is trees ha^{-1} and m_i is the fraction of the biomass per tree (W_i/N) in the ith pool that is lost when a tree dies.

The root biomass partitioning ratio is a function of the minimum and maximum root partitioning ratios (η_{Rn} and η_{Rx}) given by

$$\eta_R = \frac{\eta_{Rx}\eta_{Rn}}{\eta_{Rn} + (\eta_{Rx} - \eta_{Rn})m\varphi} \quad (A.26)$$

where, m is a linear function of FR such that

$$m = m_0 + (1 - m_0)\,FR \quad (A.27)$$

where, m_0 is the value of m on sites of poor fertility (i.e. FR = 0) (Sands and Landsberg, 2002). Therefore, partitioning between above- and below-ground biomass is influenced by nutrition, soil moisture, VPD and age.

The rest of the biomass is partitioned between the stems and foliage such that $\eta_R + \eta_S + \eta_F = 1$. Landsberg and Waring (1997) showed that the ratio η_F/η_S (denoted as p_{FS}) is an allometric function of stem diameter at breast height (B).

$$p_{FS}(B) = a_P B^{n_P} \quad (A.28)$$

where, a_p and n_p, are constants. While these constants can be derived from allometric leaf mass and stem mass equations (Landsberg and Waring, 1997), Sands and Landsberg (2002) note that after the canopy closes W_F is in a quasi-steady-state equilibrium and its relationship with B can deteriorate (note that W_F not only includes all current but also all past foliage mass, including litterfall). Therefore, to simplify parameterisation, p_{FS} is parameterised in terms of its values at B = 2 cm (p_2) and B = 20 cm (p_{20})

instead of in terms of a_p and n_p, which can instead be calculated from p_2 and p_{20} such that

$$n_p = \frac{\ln\left(p_{20}/p_2\right)}{\ln 10},\ a_p = \frac{p_2}{2^{n_p}} \tag{A.29}$$

The p_{FS} parameter is probably also sometimes influenced by stand density and competition for light (Bernardo et al., 1998; Forrester et al., 2012), and a new parameter is being developed to take this into account. An alternative approach (not included in 3-PG$_{mix}$) that has been used was to predict p_{FS} from stand basal area (Gonzalez-Benecke et al., 2014).

A.5. Species proportions and canopy cover

The proportion of a mixed-species stand that is composed of a given species is required when calculating canopy conductance, rainfall interception and density-dependent mortality. The species proportion of the ith species in a mixture containing n species can be calculated using Eq. (A.30). The species proportion (sp) is calculated in terms of different variables (e.g., L, basal area, N) depending on what the sp will be used to calculate.

$$\mathrm{sp}_{Xi} = \frac{X_i}{\sum_n^{i=1} X_i} \tag{A.30}$$

where, X is the variable that defines the species contributions (e.g., L, basal area, N).

The canopy cover, ζ, is required if Eq. (A.16) is used to predict ϕ_{pa} (as opposed to Eq. (A.19) which does not require ζ) or if wood $\delta^{13}C$ is predicted using Eq. (A.46). When the light model of Eq. (A.16) is used, the ζ is calculated using a parameter that defines the age when that species closes its canopy (t_C) (Sands, 2004a). If the age is already more than t_C then

$$\zeta = 1 \tag{A.31}$$

If the stand age is still less than t_C then

$$\zeta = \mathrm{age}/t_C \tag{A.32}$$

However, ζ then only varies with age, increasing until the canopy closes, but also needs to vary in response to any other factors that influence canopy cover, such as thinning, and in mixtures it needs to be expressed only in terms of a given species (not the total stand). Therefore, ζ is calculated as the sum of the crown projection area of all the trees of that species up to a maximum of 1 using Eq. (A.33).

$$\zeta = \min\left(1, \frac{N(K+0.25)^2}{10000}\right) \tag{A.33}$$

where, K is the crown diameter (m) and N is the number of trees ha^{-1}. Crown projection area is not calculated in the traditional way where it would be $\pi(K/2)^2$. Instead, it is estimated as a square with sides K + 0.25 m in length. The extra 0.25 m takes into account that crowns often do not touch exactly leaving some space between them due to abrasion from the movement of adjacent crowns. The calculation is based on a square not a circle because there is often some open space between crowns (which tend to be more circular than square), even in stands with closed canopies, and this space also needs to be accounted for when calculating canopy cover in mixtures.

A.6. Mortality

Density-dependent mortality is calculated using the self-thinning rule (Landsberg and Waring, 1997), which is used to determine the maximum individual tree stem mass (w_{Sx}, kg per tree) from the current number of trees per ha (N) using Eq. (A.34) (Sands and Landsberg, 2002).

$$w_{Sx} = w_{Sx1000}\left(\frac{1000}{N}\right)^{n_m} \tag{A.34}$$

where, w_{Sx1000} is the value of w_{Sx} when N = 1000 trees per ha and n_m is the exponent of the self-thinning rule. When the mean individual tree stem mass w_s (W_S/N) is greater than w_{Sx} the N will be reduced and hence w_{Sx} will increase. This is done following an iterative procedure until $w_s < w_{Sx}$. The trees that are removed are assumed to be smaller than the mean tree (for the given species), and for each tree that dies a fraction m_i of the mean biomass w_i of the ith biomass pool (stem, foliage and root) is removed (Sands, 2004a). The fractions m_i are generally less than 1 and are used in Eqs. (A.23)–(A.25) to update the values of W_F, W_R and W_S.

In mixed-species stands, the N used in Eq. (A.34) for the ith species ($N_{mix,i}$) needs to be adjusted using the N of that species (N_i) and the sp. The $N_{mix,i}$ is an estimate of what the N of the given species would be in a monoculture that has the same total stand basal area as the mixture. For density-dependent mortality sp is calculated in terms of basal area using Eq. (A.30) and $N_{mix,i}$ is calculated as

$$N_{mix,i} = \frac{N_i}{\mathrm{sp}_{\mathrm{basal\ area},i}} \tag{A.35}$$

This ignores the fact that different species have a different competitive (or facilitative) ability for a given tree size or basal area and that density-dependent mortality varies spatially and temporally with site and climatic variables. New mortality calculations that take this into account are being developed.

Mortality can also be density-independent and the density-independent mortality rate (γ_N, %) declines with age according to Eq. (A.36) (Sands, 2004a).

$$\gamma_N(t) = \gamma_{N1} + (\gamma_{N0} - \gamma_{N1})\, e^{-(\ln 2)\left(t/t_{\gamma N}\right)^{n_{\gamma N}}} \tag{A.36}$$

where, γ_{N0} and γ_{N1} are the values of γ_N in very young and mature stands, respectively, and $t_{\gamma N}$ is the age at which $\gamma_N = ½(\gamma_{N0} + \gamma_{N1})$.

A.7. Evapotranspiration and soil water balance

The soil water balance model in 3-PG operates on a monthly time step and is a balance between evapotranspiration E_T, rainfall R_P and irrigation R_{Ir}, all in mm month^{-1}

$$\Delta\theta_S = (1 - I_{RT})\, R_P + R_{Ir} - E_T \tag{A.37}$$

where, $\Delta\theta_S$ is the change in soil water and I_{RT} is the fraction of rainfall intercepted and subsequently evaporated from the canopy (Sands and Landsberg, 2002). This I_{RT} is the total for all cohorts and canopy layers in a given stand. If the $\Delta\theta_S$ results in a θ_S value in excess of the water holding capacity (θ_{Sx}) the excess water is drained off the site and assumed to have been run-off or deep drainage.

A.7.1. Rainfall interception

The calculation of I_R is based on the correlation between I_R and L (Hatton et al., 1992; Vertessy et al., 1996) such that interception I_R by the ith species (or cohort or dominance class) increases with the L of that species up to a maximum interception I_{Rx}.

$$I_R = I_{Rx} \min\left\{1, L_{mix}/L_{Ix}\right\} \times \mathrm{sp}_L \tag{A.38}$$

where, L_{Ix} is the L at which interception is a maximum (in a monoculture) for species i. In monocultures $L = L_{mix}$. In mixtures the L_{mix} of the ith species is used to adjust the L of the ith species according to the proportion of total stand L that the given species contributes (sp_{Li}, Eq. (A.30)) using Eq. (A.39). The L_{mix} is an estimate of what

the L of the given species would be in a monoculture that has the same total stand L as the mixture.

$$L_{\text{mix}} = \frac{L_i}{\text{sp}_{\text{Li}}} \tag{A.39}$$

In mixtures the total stand I_R is calculated as the sum of the I_R of all species (or cohorts or dominance classes) assuming an additive effect of mixing species (André et al., 2008). No consideration is given to which species overtop others, unlike light absorption, where vertical structure must be considered. It is important to note that this interception calculation is a considerable simplification, because interception is more accurately modelled at time scales of single rainfall events (Landsberg and Waring, 1997; Almeida et al., 2007; Feikema et al., 2010b; Almeida and Sands, 2015).

A.7.2. Canopy conductance

There are two options for predicting canopy conductance (g_c) following the same distinction used when calculating canopy quantum efficiency. Both options assume that g_c increases with L up to a maximum g_{cmax} and also change g_c in response to age, atmospheric CO_2, VPD and soil water (θ_S). The first option is the original approach used by 3-PG where the physiological modifier ϕ is calculated in the form of Eq. (A.3a) using minimum (f_θ, f_D) such that only the most limiting of VPD and soil water influence g_c (Eq. (A.40)) (Landsberg and Waring, 1997). Eq. (A.40) also includes the CO_2 modifier (Eq. (A.12)). The $L = L_{\text{mix}}$ for monocultures, and in mixtures the L_{mix} takes the species proportions into account (as previously shown in Eqs. (A.38) and (A.39)).

$$g_c = g_{\text{cmax}} \varphi f_{Cg} \min\left\{1, L_{\text{mix}}/L_{g_{\text{cmax}}}\right\} \tag{A.40}$$

where, $L_{g_{\text{cmax}}}$ is the L at which g_c is a maximum. The second option uses ϕ calculated with Eq. (A.3b) ($f_\theta \times f_D$) so that both the soil water availability and VPD modifiers will influence g_c (Eq. (A.41)). In addition, the temperature modifier for g_c (f_{gT}) is applied.

$$g_c = g_{\text{cmax}} f_\theta f_D f_{\text{AGE}} f_{gT} f_{Cg} \min\left\{1, L_{\text{mix}}/L_{g_{\text{cmax}}}\right\} \tag{A.41}$$

Note that it is assumed that either g_{cmax} (in Eqs. (A.40) and (A.41)) does not vary for a given species between monocultures and mixtures or that this effect is captured by the other variables and parameters influencing g_c.

A.7.3. Transpiration

Transpiration is predicted using the Penman–Monteith equation (Eq. (A.42)). This equation combines the two environmental drivers of evaporation, which are the supply of net radiant energy (ϕ_n) and of dry air (D_q), with the two essential controls, which are g_B, a measure of the mixing power of the atmosphere, and g_c the main physiological control exerted by the trees (Landsberg and Gower, 1997).

$$\lambda E = \frac{s\emptyset_n + \lambda \rho_a g_B D_q}{s + 1 + g_B/g_c} \tag{A.42}$$

λ is the latent heat of vapourisation of water (2.46×10^6 J kg^{-1}). The total net radiation ϕ_n is calculated from solar radiation ϕ_s (MJ m^{-2} day^{-1}) as $R_n = Q_a + Q_b R_s$ W m^{-2}, where Q_a and Q_b are parameters that are often −90 and 0.8, respectively. s is the slope of saturated vapour pressure versus temperature curve at a temperature of 20 °C (2.2). ρ_a is air density (1.2 kg m^{-3}), g_B is the aerodynamic conductance above the canopy and is assumed to be 0.2 m s^{-1} (Landsberg and Gower, 1997 p. 76; Sands and Landsberg, 2002) and D_q is the specific saturation deficit ($6.22 \times 10^{-4} \times$ VPD).

Variables such as g_B and VPD are likely to vary at different depths within the canopy (Landsberg and Sands, 2010, p. 32) and each species i may receive a different net radiation ϕ_{ni} depending on their positions within the canopy as well as the stand density. Therefore, g_B, VPD and ϕ_n used by Eq. (A.42) can either be the same for all species within the stand, and equal to values above the canopy, or they can be predicted for the given species based on its position within the canopy and the vertical distribution of L (option E in Table 1). The ϕ_{ni} for an individual species is calculated using the same extinction coefficient as PAR such that $\phi_{ni} = \phi_n \times \phi_{\text{pai}}/\phi_p$ (Wallace, 1997), where ϕ_{pai} is from Eq. (A.19) and considers the horizontal and vertical heterogeneity of the canopy. If this within-canopy climatic variation is used the same within-canopy VPD value is used to calculate the f_D modifier (Eq. (A.8)) and will therefore also influence the calculation of P_G and g_c. If the focal species is the tallest species in the forest then the g_B and VPD will not be changed, and therefore, for a monoculture both options will give exactly the same predictions. Also, when this second option (option E in Table 1) is used the soil evaporation is calculated, whereas this is not calculated when within-canopy climate is not considered.

The aerodynamic resistance ($r_a = 1/g_B$, s m^{-1}) at a height of h metres is calculated as

$$r_a(h) = \frac{1}{g_B} + \left(r_a^{soil} - \frac{1}{g_B}\right) e^{-(\ln 2)\left(h/h_{0.5}\right)^2} \tag{A.43}$$

where, r_a^{soil} is the aerodynamic resistance above the soil estimated as 5 × total L, which is the sum of the L of all species in the forest. $h_{0.5}$ is half the height of the tallest species within the forest.

Soil conductance g_{soil} is calculated following (Soares and Almeida, 2001)

$$g_{\text{soil}} = g_{\text{soilx}} \frac{\theta}{\theta_{\text{max}}} \tag{A.44}$$

where g_{soilx} is the maximum g_{soil} and θ_{max} is the maximum soil θ. The g_{soilx} can be input, otherwise the default is 0.0025 m s^{-1}.

The VPD within the canopy (D_c) is calculated using Eq. (A.45).

$$D_c = D \times e^{\frac{L_{\text{above}} \times -\ln 2}{L_{50}}} \tag{A.45}$$

where L_{50} is the (monoculture) L that leads to a 50% reduction in D (default = 5) for the given species, and L_{above} is the L of all layers above the layer in which the given species is in. If the given species is positioned in the lower part of the given layer, $\frac{h_{m,i}}{h_m} < 1$ (see Eq. (A.20)) then the L_{above} for that species also includes $(1 - \frac{h_{m,i}}{h_m}) \times L$ of the given layer. This means that in mixtures, as soon as another species is taller than a given species its D_c will drop and so will its transpiration. The D_c above the soil is also calculated using Eq. (A.45) and assuming $L_{50} = 5$.

A.8. $\delta^{13}C$ of wood

The $\delta^{13}C$ of wood is predicted using the approach of Wei et al. (2014a,b). Predictions of $\delta^{13}C$ have no influence on any of the predictions of other variables within 3-PG$_{\text{mix}}$ but they can be useful in the parameterisation and calibration processes, especially where there are no empirical P_G and transpiration data available (Wei et al., 2014b). An example used by Wei et al. is when the model incorrectly predicts P_G. In this case, "tuning" the allocation parameters can still enable 3-PG to accurately predict stem mass, volume, basal area and L, however, it would be doing so for the wrong physiological reasons.

The $\delta^{13}C$ of new photosynthate in C_3 plants ($\delta^{13}C_p$) can be estimated using Eq. (A.46) (Farquhar et al., 1982; Wei et al., 2014a,b).

$$\delta^{13}C_p = \delta^{13}C_a - a - (b - a)\left(1 - \frac{A}{c_a g}\right) \tag{A.46}$$

The $\delta^{13}C_a$ is the isotopic composition of air, a is the fractionation against ^{13}C in diffusion through air (4.4‰), b is the enzymatic fractionation by Rubisco (27‰), c_a is the molar fraction of CO_2 in

the air, A is net assimilation rate (mol C m^{-2} s^{-1}) and g is conductance to the diffusion of CO_2 (mol C m^{-2} s^{-1}). g is converted from g_c (m s^{-1}) assuming a ratio of diffusivities of CO_2 to water vapour in air of 0.66, and A is converted from GPP. The canopy cover (ζ, Eqs. (A.31)–(A.33)) is used to convert g_c to g, because the former is calculated on the assumption of uniform leaf distribution across the land area, while g only needs the ground area covered by the leaves. It is assumed that the difference between mean annual $\delta^{13}C_p$ and $\delta^{13}C$ of tree rings ($\delta^{13}C_s$) is constant (ε_{sp}) for all months and years and therefore $\delta^{13}C_s$ is calculated using Eq. (A.47).

$$\delta^{13}C_s = \delta^{13}C_p + \varepsilon_{sp} \tag{A.47}$$

A.9. Litterfall and deciduous species

Monthly litterfall (Mg ha^{-1} $month^{-1}$) is calculated as $\gamma_F W_F$, where the litterfall rate, γ_F ($month^{-1}$), is the fraction of W_F that falls as litter per month, and increases from γ_{F0} in young stands to γ_{F1} in older stands. For example, Landsberg et al. (2003) calculate γ_F for a stand where average leaf lifespan is 3 years, so the loss is about 33% per year, which would be equivalent to 0.33/12 = 0.0275 = γ_F. The age-dependency of γ_F is given by

$$\gamma_F(t) = \frac{\gamma_{F1}\gamma_{F0}}{\gamma_{F0} + (\gamma_{F1} - \gamma_{F0})\, e^{-(t/t_{\gamma F})\ln(1+\gamma_{F1}/\gamma_{F0})}} \tag{A.48}$$

where, $t_{\gamma F}$ is the age at which the litterfall rate is ½(γ_{F0} + γ_{F1}) (Sands and Landsberg, 2002). Litterfall will be influenced by all factors that influence W_F (and hence P_G and partitioning) as well as thinning, defoliation or other disturbances, but it is assumed that none of those factors influence the γ_F. For deciduous species the γ_F only includes the litterfall (if there is any) that occurs during the growing season and does not include the large litterfall event that occurs at the end of the growing season.

There are two options for controlling the timing of the large litterfall event that occurs for deciduous species. This also defines when they become inactive in terms of light absorption, assimilation, transpiration, canopy rainfall interception and hence their competitive effect on other species. The first option is to provide a T_{min} below (or T_{max} above) which the f_T (Eq. (A.5)) will result in zero P_G. This approach was used for *Betula platyphylla* forests (Potithep and Yasuoka, 2011). However, this approach only stops the trees from functioning during the cold (or hot) period; it does not cause the loss of any leaves (L is unchanged) and hence no assimilates are required to rebuild the canopy in spring because the W_F has not been lost and simply becomes active again. Another potential problem is that the timing of leaf fall or bud break may also be influenced by variables other than temperature, so temperature alone may not be enough to determine the dormant season. Similarly, the dormant season can also be during the dry season or even during the wet season for some species (Roupsard et al., 1999). To deal with this, the second option for defining the growing season is that the month (1–12) when the trees produce their leaves at the start of the season ($leaf_P$) and the month when they lose their leaves ($leaf_L$) must be provided. It is then assumed that all existing W_F is lost at the start of the month of leaf fall and that the WF that existed in the month prior to leaf fall will be produced again at the end of the first month of the next growing season ($leaf_P$). However, no further growth occurs until the tree has assimilated a NPP equal to the W_F, while losses (litterfall and roots) continue to occur as this W_F is being rebuilt. It is assumed that after W_F has been rebuilt the W_S, W_R and W_F will all be produced as usual. After deciduous species have rebuilt their W_F it is conceivable (but not implemented into 3-PG_{mix}) that there may be very little NPP allocated to W_F for the rest of the growing season, such that most NPP goes to W_S and W_R. However, this potential change in partitioning is currently not taken into account in 3-PG_{mix}. Similarly, the increase or decrease in L at the beginning and end of a growing season does not occur instantly from one month to the next and occurs gradually over a month or so (Norby et al., 2003; Oishi et al., 2008) and four parameters (not two) may be necessary to define the start and end times of leaf growth and the start and end times of leaf shedding.

A.10. Bias corrections and diameter distributions

3-PG_{mix} calculates several variables using allometric equations. One of these is the partitioning variable p_{FS} which is calculated from mean tree diameter (B) using Eq. (A.28). Another example is when B is calculated from w_s by inverting Eq. (A.65). However, these relationships are usually not linear so this approach will lead to biased predictions of p_{FS} or B due to Jensen's Inequality (Duursma and Robinson, 2003). That is, the mean of a function is not the same as the function of the mean (Duursma and Robinson, 2003). Biased predictions of p_{FS} will cause partitioning errors while biased predictions of B will lead to biased predictions of all variables predicted from B that are not linearly related to B, which might include height, crown diameter, volume, basal area etc. Some of these B-derived variables (e.g. volume) are only outputs and have no influence on any of the processes predicted by 3-PG_{mix}, however, variables such height and crown diameter are required by the light model described by Eq. (A.19) and height is required if transpiration (and hence P_G) is calculated using the within-canopy climatic VPD and aerodynamic conductance (Eq. (A.43)). Variables such as basal area are required in self-thinning calculations (e.g., Eq. (A.35) for mixed-species stands). Therefore it is important that the bias is accounted for (Weiskittel et al., 2010).

Duursma and Robinson (2003) showed that the relative bias resulting from calculating a variable such as mean p_{FS} from B (Eq. (A.28)), which could be expressed as $p_{FS} = a_b B^{b_b}$, where a and b are constants, can be given by

$$\mathrm{BIAS}_{rel} = \frac{1}{2}\left[b_b(b_b - 1)\right]\mathrm{CV}^2 \tag{A.49}$$

where, CV is the coefficient of variation in B and is obtained from the 3-PG_{mix} calculations from the previous month. A positive relative bias indicates how much the true value of a given variable will have been underestimated (Duursma and Robinson, 2003), such that the true value = biased value × (1 + BIAS_{rel}). The same equation can be applied to any other relationship where B is used to estimate tree height, stem volume, basal area (basal area $\propto B^2$), crown diameter and live-crown length (Eqs. (A.61)–(A.64)). It can also be applied when mean w_S is used to predict B by inverting Eq. (A.65), in which case the exponent is also inverted such that $B \propto w_S^{1/b_b}$ and b_b in Eq. (A.49) is replaced with $1/b_b$ (Duursma and Robinson, 2003).

The use of Eq. (A.49) requires a measure of the CV of the explanatory variable. In 3-PG_{mix} the CV can be provided as an input or calculated from Weibull distributions (of B and w_s) whose location (loc), shape (sh) and scale (sc) parameters are provided by the user. If the location is not provided, but the shape and scale are (2-parameter Weibull distribution), then location will be predicted using Eq. (A.50).

The expected value $E(x)$ and the variance var(x) of a Weibull function can be calculated from its location, scale and shape parameters.

$$E(x) = \mathrm{loc} + \mathrm{sc}\Gamma\left(1 + \frac{1}{\mathrm{sh}}\right) \tag{A.50}$$

$$var(x) = sc^2 \left[\Gamma\left(1 + \frac{2}{sh}\right) - \left(\Gamma\left(1 + \frac{1}{sh}\right)\right)^2 \right] \quad (A.51)$$

The B and w_s distributions are described using 3-parameter Weibull probability distribution functions

$$N_{class} = \left(\left(\frac{sh}{sc}\right) \times \left(\frac{sizeclass - loc}{sc}\right)^{(sh-1)} \times e^{-\left(\frac{sizeclass-loc}{sc}\right)^{sh}} \right) \times N \quad (A.52)$$

where, N_{class} is the number of trees per ha within a given B or w_s class. The sizeclass is the diameter or w_s size class from the smallest size class (sizeclass = 1) to the largest size class in (strictly) 1-cm intervals for B or 10-kg intervals for w_s. The location, scale and shape parameters must all be greater than zero. If sh = 3.6 the distribution is approximately normal, while if sh < 3.6 the distribution is positively skewed (to the right) and if sh > 3.6 the distribution is negatively skewed (to the left). Several previous studies have successfully used Weibull parameters to describe B distributions in 3-PG (Landsberg et al., 2005; Wang et al., 2011).

Eq. (A.53) is used to convert the sizeclass into the units of the distribution variable (B or w_s).

$$\text{Actual class} = \text{classwidth}\,(1 + \text{sizeclass} + \text{location}) \quad (A.53)$$

where, actual class is the mid-point of the given size class in cm (B) or kg (w_s), classwidth is the width of each size class, which is strictly 1-cm for B and 10-kg intervals for w_s.

There are three input options regarding the distributions. One is to ignore the bias. The second option allows the user to enter the intercept (a_{BCV}) and slope (b_{BCV}) of the relationship between age and CV of the B distribution or the w_s distribution (intercept = a_{wCV} and slope = b_{wCV}). If this option is chosen but these parameters are not provided then it is assumed that the CV increases from $b_{BCV} = b_{wCV} = 0.15$ at age 0 to 0.45 at the maximum stand age (t_x, Eq. (A.10)), such that $b_{BCV} = b_{wCV} = (0.45 - 0.15)/t_x$. The third option is to provide the location, scale and shape parameters of the Weibull distribution for B or w_s. These parameters can be constant or vary according to empirical equations provided by the user (Eqs. (A.54)–(A.59)).

$$loc_B = loc_{B0} + loc_{BB}B + loc_{Bh}h + loc_{Bt}Age + loc_{BC}C \quad (A.54)$$

$$sc_B = sc_{B0} + sc_{BB}B + sc_{Bh}h + sc_{Bt}Age + sc_{BC}C \quad (A.55)$$

$$sh_B = sh_{B0} + sh_{BB}B + sh_{Bh}h + sh_{Bt}Age + sh_{BC}C \quad (A.56)$$

$$loc_w = loc_{w0} + loc_{wB}B + loc_{wh}h + loc_{wt}Age + loc_{wC}C \quad (A.57)$$

$$sc_w = sc_{w0} + sc_{wB}B + sc_{wh}h + sc_{wt}Age + sc_{wC}C \quad (A.58)$$

$$sh_w = sh_{w0} + sh_{wB}B + sh_{wh}h + sh_{wt}Age + sh_{wC}C \quad (A.59)$$

where, loc_{Bx}, sc_{Bx} and sh_{Bx} are fitted parameters for the B distributions, loc_{wx}, sc_{wx} and sh_{wx} are fitted parameters for the w_s distributions and C is a competition index calculated using Eq. (A.60). The C is the sum of the products of the basal area (BA, $m^2\,ha^{-1}$) and the wood basic density (ρ, $Mg\,m^{-3}$) of each of n species.

$$C = \sum_{i=1}^{n} BA_i \times \rho_i \quad (A.60)$$

It is assumed that ρ provides an estimate of the competitive ability of each species per unit of its basal area.

A.11. Stand-level variables

Allometric equations are used to predict mean tree height (h, m), live-crown length (h_L, m), crown diameter (K, m), basal area (ba, m^2) and tree volume.

$$h = a_H B^{n_{HB}} C^{n_{HC}} \quad (A.61)$$

$$h_L = a_{H_L} B^{n_{HLB}} L^{n_{HLL}} C^{n_{HLC}} \quad (A.62)$$

$$K = a_K B^{n_{KB}} h^{n_{KH}} C^{n_{KC}} \quad (A.63)$$

$$ba = \pi B^2/40000 \quad (A.64)$$

$$w_S = a_S B^{n_S} \quad (A.65)$$

where, all a_x or n_x parameters are constants. All equations must have an "a_x" parameter, but the inclusion of the other parameters is optional and will depend on whether they are deemed necessary for the given species. Note that w_s (Eq. (A.65)) is all above-ground biomass that is not foliage (stem + bark + branch). Stand basal area (BA, $m^2\,ha^{-1}$) is calculated as ba × N. There are two options for calculating stand volume (V_S, $m^3\,ha^{-1}$) and when both are provided Eq. (A.66) will be used rather than Eq. (A.67).

$$V_S = a_V B^{n_{VB}} h^{n_{VH}} \left(B^2 h\right)^{n_{VBH}} \times N \quad (A.66)$$

$$V_S = (1 - p_{BB})\, W_S/\rho \quad (A.67)$$

where, p_{BB} is the fraction of w_s that is branch and bark and, with Eq. (A.66) generally preferred over Eq. (A.67), which needs to account for temporal changes in p_{BB} and w_s (Sands and Landsberg, 2002). Volume can be output as the currently existing (standing) volume, cumulative extracted volume (all volume thinned so far during the rotation), extracted volume for the latest thinning event, total cumulative volume (standing + extracted + mortality) and mean annual volume increment (total cumulative volume/age).

The ρ increases with age such that

$$p_{BB}(t) = \rho_1 + (\rho_0 - \rho_1)\, e^{-(\ln 2)(t/t_\rho)} \quad (A.68)$$

where, ρ_0 and ρ_1 are the minimum (young trees) and maximum (older trees) values of ρ, respectively, and t_ρ is the age at which $\rho = \frac{1}{2}(\rho_0 + \rho_1)$ (Sands, 2004a).

The p_{BB} declines with age such that

$$p_{BB}(t) = p_{BB1} + (p_{BB0} - p_{BB1})\, e^{-(\ln 2)(t/t_{BB})} \quad (A.69)$$

where, p_{BB0} and p_{BB1} are the values of p_{BB} for very young and for mature stands, respectively, and t_{BB} is the age at which $p_{BB} = \frac{1}{2}(p_{BB0} + p_{BB1})$ (Sands, 2004a).

Eqs. (A.61)–(A.66) are all corrected for the bias associated with using mean B or w_s using Eq. (A.49). Volume is often predicted using only B^2h and this relationship is usually close to linear, and so it is assumed that bias corrections are not required. It is assumed that the exponents of the other explanatory variables in Eqs. (A.61)–(A.64) (h, L, CL) are also often close to linear and bias corrections are not currently made for these variables by 3-PG_{mix}.

Finally, if outputs for the "x" largest-B crop trees per ha are required, Eq. (A.52) is used to construct a B-distribution with 1-cm size intervals, and is used to predict the W_S, volume, mean B, h and BA of the largest "x" trees per ha. This is useful for predicting mean dominant height, which is often the largest 100 trees per ha. These crop tree calculations can only be done if Weibull parameters have been provided. Also, no values are provided until the location parameter is >0.01 to avoid overestimating the crop tree values.

Appendix B.

See Fig. B.1.

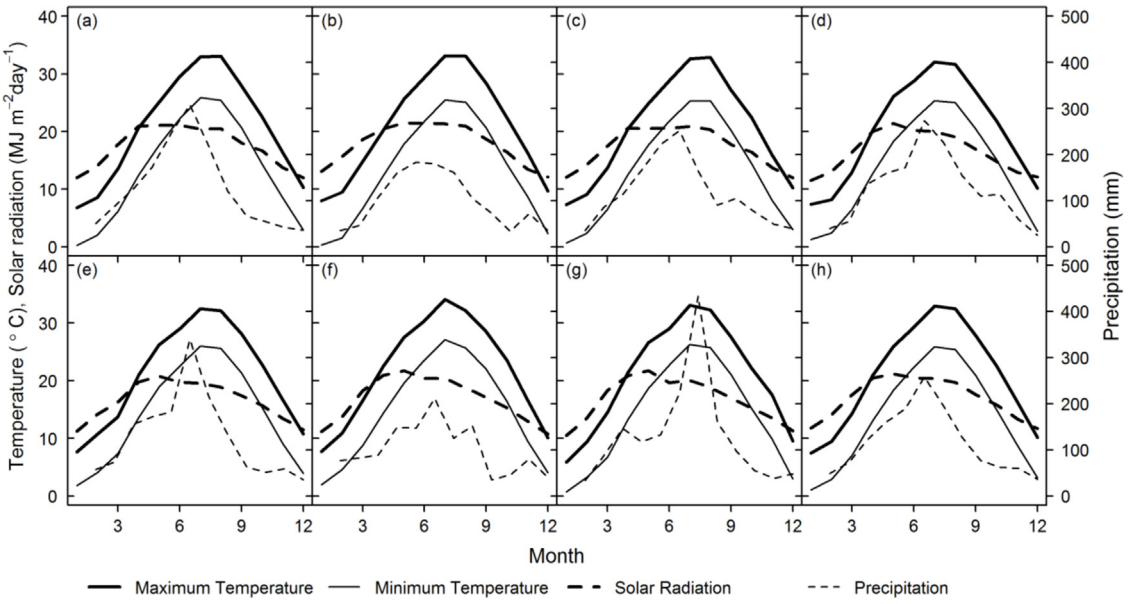

Fig. B.1. Mean monthly climate for each decade of available data including the 1950s (a), 1960s (b), 1970s (c), 1980s (d), 1990s (e), 2000s (f), 2010s (g) and the long-term average from 1951 until 2012 (h). Data obtained from the GHCN (Menne et al., 2012; NOAA, 2013).

References

Almeida, A.C., Sands, P.J., 2015. Improving the ability of 3-PG to model the water balance of forest plantations in contrasting environments. Ecohydrology.

Almeida, A.C., Soares, J.V., Landsberg, J.J., Rezende, G.D., 2007. Growth and water balance of *Eucalyptus grandis* hybrid plantations in Brazil during a rotation for pulp production. Forest Ecol. Manag. 251, 10–21.

Almeida, A.C., Siggins, A., Batista, T.R., Beadle, C., Fonseca, S., Loos, R., 2010. Mapping the effect of spatial and temporal variation in climate and soils on *Eucalyptus* plantation production with 3-PG, a process-based growth model. Forest Ecol. Manag. 259, 1730–1740.

Almeida, A.C., Sands, P.J., Bruce, J., Siggins, A.W., Leriche, A., Battaglia, M., Batista, T.R., 2009. Use of a spatial process-based model to quantify forest plantation productivity and water use efficiency under climate change scenarios. In: Interfacing Modelling and Simulation with Mathematical and Computational Sciences. Modelling and Simulation Society of Australia and New Zealand and International Association for Mathematics and Computers in Simulation, Cairns, Australia.

Almeida, A.C.D., Landsberg, J.J., Sands, P.J., 2004a. Parameterisation of 3-PG model for fast-growing Eucalyptus grandis plantations. Forest Ecol. Manag. 193, 179–195.

Almeida, A.C.D., Landsberg, J.J., Sands, P.J., Ambrogi, M.S., Fonseca, S., Barddal, S.M., Bertolucci, F.L., 2004b. Needs and opportunities for using a process-based productivity model as a practical tool in Eucalyptus plantations. Forest Ecol. Manag. 193, 167–177.

Amichev, B.Y., Johnston, M., Rees, K.C.J.V., 2010. Hybrid poplar growth in bioenergy production systems: biomass prediction with a simple process-based model (3-PG). Biomass Bioenergy 34, 687–702.

Amichev, B.Y., Hangs, R.D., Rees, K.C.J.V., 2011. A novel approach to simulate growth of multi-stem willow in bioenergy production systems with a simple process-based model (3-PG). Biomass Bioenergy 35, 473–488.

Amoroso, M.M., Turnblom, E.C., 2006. Comparing productivity of pure and mixed Douglas-fir and western hemlock plantations in the Pacific Northwest. Can. J. Forest Res. 36, 1484–1496.

André, F., Jonard, M., Ponette, Q., 2008. Precipitation water storage capacity in a temperate mixed oak-beech canopy. Hydrol. Process. 22, 4130–4141.

Andrén, O., Kätterer, T., 1997. ICBM: the introductory carbon balance model for exploration of soil carbon balance. Ecol. Appl. 7, 1226–1236.

Battaglia, M., Sands, P.J., 1998. Process-based forest productivity models and their application in forest management. Forest Ecol. Manag. 102, 13–32.

Battaglia, M., Almeida, A.C., O'Grady, A.P., Mendham, D., 2007. Process-based model in Eucalyptus plantation management: reality and perspectives. Boletín del CIDEU 3, 189–205 (ISSN 1885-5237).

Bernardo, A.L., Reis, M.G.F., Reis, G.G., Harrison, R.B., Firme, D.J., 1998. Effect of spacing on growth and biomass distribution in *Eucalyptus camaldulensis, E. pellita* and *E. urophylla* plantations in southeastern Brazil. Forest Ecol. Manag. 104, 1–13.

Binkley, D., Campoe, O.C., Gspaltl, M., Forrester, D.I., 2013. Light absorption and use efficiency in forests: why patterns differ for trees and forests. Forest Ecol. Manag. 288, 5–13.

Bugmann, H., 2001. A review of forest gap models. Clim. Change 51, 259–305.

Cannell, M.G.R., Milne, R., Shepphard, L.J., Unsworth, M.A., 1987. Radiation interception and productivity of willow. J. Appl. Ecol. 24, 261–278.

Charbonnier, F., Maire, G.L., Dreyer, E., Casanoves, F., Christina, M., Dauzat, J., Eitel, J.U.H., Vaast, P., Vierling, L.A., Roupsard, O., 2013. Competition for light in heterogeneous canopies: application of MAESTRA to a coffee (*Coffea arabica* L.) agroforestry system. Agric. Forest Meteorol. 181, 152–169.

Chen, G.-S., Yang, Y.-S., Xie, J.-S., Guo, J.-F., Gao, R., Qian, W., 2005. Conversion of a natural broad-leafed evergreen forest into pure plantation forests in a subtropical area: effects on carbon storage. Ann. Forest Sci. 62, 659–668.

Chen, G.-S., Yang, Z.-J., Gao, R., Xie, J.-S., Guo, J.-F., Huang, Z.-Q., Yang, Y.-S., 2013. Carbon storage in a chronosequence of Chinese fir plantations in southern China. Forest Ecol. Manag. 300, 68–76.

Condés, S., Rio, M.D., Sterba, H., 2013. Mixing effect on volume growth of *Fagus sylvatica* and *Pinus sylvestris* is modulated by stand density. Forest Ecol. Manag. 292, 86–95.

Delignette-Muller, M. L., Pouillot, R., Denis, J.-B., Dutang, C., 2014. fitdistrplus: Help to Fit of a Parametric Distribution to Non-Censored or Censored Data.

Duursma, R.A., Robinson, A.P., 2003. Bias in the mean tree model as a consequence of Jensen's inequality. Forest Ecol. Manag. 186, 373–380.

Duursma, R.A., Mäkelä, A., 2007. Summary models for light interception and light-use efficiency of non-homogeneous canopies. Tree Physiol. 27, 859–870.

Dye, P., 2005. Final Report: A New Decision Support Software Tool For Tree Growers And Water Resource Managers: Harnessing Physiological Information to Improve Productivity And Water Use Assessment Of Forest Plantations. National Research Foundation, Pretoria, South Africa (Innovation Fund Project 23407).

Dye, P.J., 2001. Modelling growth and water use in four *Pinus patula* stands with the 3-PG model. S. Afr. Forest J. 191, 53–63.

Esprey, L.J., Sands, P.J., Smith, C.W., 2004. Understanding 3-PG using a sensitivity analysis. Forest Ecol. Manag. 193, 235–250.

Fan, H.B., Liu, W.F., Wu, J.P., Li, Y.Y., Yuan, Y.H., Liao, Y.C., Huang, R.Z., Su, X.Q., 2013. Ecosystem carbon pools in mixed stands of Hardwood species and Masson Pine. J. Trop. Forest Sci. 25, 154–165.

Farquhar, G.D., Oleary, M.H., Berry, J.A., 1982. On the relationship between carbon isotope discrimination and the inter-cellular carbon-dioxide concentration in leaves. Aust. J. Plant Physiol. 9, 121–137.

Feikema, P.M., Morris, J.D., Beverly, C.R., Lane, P.N.J., Baker, T.G.,2010a. Using 3PG+ to simulate long term growth and transpiration in Eucalyptus regnans forests. In: International Congress on Environmental Modelling and Software: Modelling for Environment's Sake. International Environmental Modelling and Software Society (iEMSs), Ottawa, Canada.

Feikema, P.M., Morris, J.D., Beverly, C.R., Collopy, J.J., Baker, T.G., Lane, P.N.J., 2010b. Validation of plantation transpiration in south-eastern Australia estimated using the 3PG+ forest growth model. Forest Ecol. Manag. 260, 663–678.

Forrester, D.I., 2014a. The spatial and temporal dynamics of species interactions in mixed-species forests: From pattern to process. Forest Ecol. Manag. 312, 282–292.

Forrester, D.I., 2014b. A stand-level light interception model for horizontally and vertically heterogeneous canopies. Ecol. Model. 276, 14–22.

Forrester, D.I., Collopy, J.J., Beadle, C.L., Baker, T.G., 2012. Interactive effects of simultaneously applied thinning, pruning and fertiliser application treatments on growth, biomass production and crown architecture in a young *Eucalyptus nitens* plantation. Forest Ecol. Manag. 267, 104–116.

Forrester, D.I., Guisasola, R., Tang, X., Albrecht, A.T., Dong, T.L., le Maire, G., 2014. Using a stand-level model to predict light absorption in stands with vertically and horizontally heterogeneous canopies. Forest Ecosyst. 1, 17.
Garber, S.M., Maguire, D.A., 2004. Stand productivity and development in two mixed-species spacing trials in the Central Oregon Cascades. Forest Sci. 50, 92–105.
Gonzalez-Benecke, C.A., Jokela, E.J., Cropper Jr., W.P., Bracho, R., Leduc, D.J., 2014. Parameterization of the 3-PG model for *Pinus elliottii* stands using alternative methods to estimate fertility rating, biomass partitioning and canopy closure. Forest Ecol. Manag. 327, 55–75.
González-García, M., Almeida, A. C., Hevia, A., Majada, J., Beadle, C. L., in press. Application of a process-based model for predicting the productivity of Eucalyptus nitens bioenergy plantations in Spain. GCB Bioenergy.
Grimm, V., 1999. Ten years of individual-based modelling in ecology: what have we learned and what could we learn in the future? Ecol. Model. 115, 129–148.
Guisasola, R., 2014. Allometric Biomass Equations And Crown Architecture In Mixed-Species Forests Of Subtropical China, Masters Thesis. Albert-Ludwigs University of Freiburg, Freiburg.
Guisasola, R., Tang, X., Bauhus, J., Forrester, D.I., 2015. Intra- and inter-specific differences in crown architecture in Chinese subtropical mixed-species forests. Forest Ecol. Manag. 353, 164–172.
Härkönen, S., Pulkkinen, M., Duursma, R., Mäkelä, A., 2010. Estimating annual GPP, NPP and stem growth in Finland using summary models. Forest Ecol. Manag. 259, 524–533.
Hatton, T.J., Walker, J., Dawes, W.R., Dunin, F.X., 1992. Simulations of hydroecological responses to elevated CO_2 at the catchment scale. Aust. J. Bot. 40, 679–696.
He, Y., Qin, L., Li, Z., Liang, X., Shao, M., Tan, L., 2013. Carbon storage capacity of monoculture and mixed-species plantations in subtropical China. Forest Ecol. Manag. 295, 193–198.
Headlee, W.L., Zalesny Jr., R.S., Donner, D.M., Hall, R.B., 2013. Using a process-based model (3-PG) to predict and map hybrid poplar biomass productivity in Minnesota and Wisconsin, USA. BioEnergy Res. 6, 196–210.
Huang, Y., Li, X., Zhang, Z., He, C., Zhao, P., You, Y., Mo, L., 2011. Seasonal changes in *Cyclobalanopsis glauca* transpiration and canopy stomatal conductance and their dependence on subterranean water and climatic factors in rocky karst terrain. J. Hydrol. 402, 135–143.
Janssen, P.H.M., Heuberger, P.S.C., 1995. Calibration of process-oriented models. Ecol. Model. 83, 55–66.
Jarvis, P.G., 1976. The interpretation of the variations in leaf water potential and stomatal conductance round in canopies in the field. Philos. Trans. R. Soc. Lond. B 273, 593–610.
Johnsen, K., Samuelson, L., Teskey, R., McNulty, S., Fox, T., 2001. Process models as tools in forestry research and management. Forest Sci. 47, 2–8.
Kang, W.X., Xiong, Z.X., He, J.N., Li, J., 2012. The energy storage and its distribution in 11-year-old chinese fir plantations in Huitong and Zhuting. Acta Ecol. Sin. 32, 6901–6908.
Kirnbauer, M.C., Baetz, B.W., Kenney, W.A., 2013. Estimating the stormwater attenuation benefits derived from planting four monoculture species of deciduous trees on vacant and underutilized urban land parcels. Urban For. Urban Green. 12, 401–407.
Korzukhin, M.D., TerMikaelian, M.T., Wagner, R.G., 1996. Process versus empirical models: which approach for forest ecosystem management? Can. J. Forest Res. 26, 879–887.
Lai, J., Yang, B., Lin, D., Kerkhoff, A.J., Ma, K., 2013. The allometry of coarse root biomass: log-transformed linear regression or nonlinear regression? PLoS One 8, e77007.
Landsberg, J., 2003. Modelling forest ecosystems: state of the art, challenges, and future directions. Can. J. Forest Res. 33, 385–397.
Landsberg, J., Sands, P., 2010. Physiological ecology of forest production: Principles, processes and models. Elsevier, Amsterdam.
Landsberg, J., Mäkelä, A., Sievänen, R., Kukkola, M., 2005. Analysis of biomass accumulation and stem size distributions over long periods in managed stands of *Pinus sylvestris* in Finland using the 3-PG model. Tree Physiol. 25, 781–792.
Landsberg, J.J., Waring, R.H., 1997. A generalised model of forest productivity using simplified concepts of radiation-use efficiency, carbon balance and partitioning. Forest Ecol. Manag. 95, 209–228.
Landsberg, J.J., Gower, S.T., 1997. Applications of Physiological Ecology to Forest Management. Academic Press, San Diego.
Landsberg, J.J., Waring, R.H., Coops, N.C., 2003. Performance of the forest productivity model 3-PG applied to a wide range of forest types. Forest Ecol. Manag. 172, 199–214.
le Maire, G., Nouvellon, Y., Christina, M., Ponzoni, F.J., Gonçalves, J.L.M., Bouillet, J.-P., Laclau, J.-P., 2013. Tree and stand light use efficiencies over a full rotation of single- and mixed-species *Eucalyptus grandis* and *Acacia mangium* plantations. Forest Ecol. Manag. 288, 31–42.
Liu, Y. 2009. Planting technology of Chinese fir (Bachelor thesis, in Chinese) Jiangxi Environmental Engineering Vocational College, Ganzhou.
López-Serrano, F.R., Martínez-García, E., Dadi, T., Rubio, E., García-Morote, F.A., Lucas-Borja, M.E., Andrés-Abellán, M., 2015. Biomass growth simulations in a natural mixed forest stand under different thinning intensities by 3-PG process-based model. Eur. J. Forest Res. 134, 167–185.
McMurtrie, R.E., Wolf, L., 1983. A model of competition between trees and grass for radiation, water and nutrients. Ann. Bot. 52, 449–458.
Medlyn, B.E., 2004. A MAESTRO Retrospective. In: Mencuccini, M., Moncrieff, J., McNaughton, K., Grace, J. (Eds.), Forests at the Land-Atmosphere Interface. CABI Publishing, Wallingford UK, pp. 105–122.
Meng, J., Lu, Y., Zeng, J., 2014. Transformation of a degraded *Pinus massoniana* plantation into a mixed-species irregular forest: impacts on stand structure and growth in Southern China. Forests 5, 3199–3221.
Menne, M.J., Durre, I., Vose, R.S., Gleason, B.E., Houston, T.G., 2012. An overview of the Global Historical Climatology Network-Daily Database. J. Atmos. Ocean. Technol. 29, 897–910.
Miehle, P., Battaglia, M., Sands, P.J., Forrester, D.I., Feikema, P.M., Livesley, S.J., Morris, J.D., Arndt, S.K., 2009. A comparison of four process-based models and a statistical regression model to predict growth of *Eucalyptus globulus* plantations. Ecol. Model. 220, 734–746.
Monserud, R.A., 2003. Evaluating forest models in a sustainable forest management context. For. Biometry Model. Inf. Sci. 1, 35–47.
NOAA, 2013. National Oceanic and Atmospheric Administration, Department of Commerce, USA, 2013. National Climatic Data Center. ⟨http://www.ncdc.noaa.gov⟩ (accessed 12.11.13.).
Norby, R.J., Sholtis, J.D., Gunderson, C.A., Jawdy, S.S., 2003. Leaf dynamics of a deciduous forest canopy: no response to elevated CO_2. Oecologia 136, 574–584.
Oishi, A.C., Oren, R., Stoy, P.C., 2008. Estimating components of forest evapotranspiration: A footprint approach for scaling sap flux measurements. Agric. Forest Meteorol. 148, 1719–1732.
Pan, W., Tian, D., Chen, X., Wen, S., 1989. Hydrological processes and nutrient dynamics of Chinese fir ecosystems in subtropical zone. J. Central South For. Univ. 9, 1–10.
Paul, K., Polglase, P., Snowdon, P., Theiveyanathan, T., Raison, J., Grove, T., Rance, S., 2006. Calibration and uncertainty analysis of a carbon accounting model to stem wood density and partitioning of biomass for *Eucalyptus globulus* and *Pinus radiata*. New Forests 31, 513–533.
Peng, C., 2000. Growth and yield models for uneven-aged stands: past, present and future. Forest Ecol. Manag. 132, 259–279.
Pérez-Cruzado, C., Muñoz-Sáez, F., Basurco, F., Riesco, G., Rodríguez-Soalleiro, R., 2011. Combining empirical models and the process-based model 3-PG to predict *Eucalyptus nitens* plantations growth in Spain. Forest Ecol. Manag. 262, 1067–1077.
Potithep, S., Yasuoka, Y., 2011. Application of the 3-PG model for gross primary productivity estimation in deciduous broadleaf forests: a study area in Japan. Forests 2, 590–609.
Pretzsch, H., Forrester, D.I., Rötzer, T., 2015. Representation of species mixing in forest growth models. A review and perspective. Ecol. Model. 313, 276–292.
R Core Team. 2013. R: A language and environment for statistical computing. R Foundation for Statistical Computing, Vienna, Austria. ⟨http://www.R-project.org/⟩.
Richards, A.E., Forrester, D.I., Bauhus, J., Scherer-Lorenzen, M., 2010. The influence of mixed tree plantations on the nutrition of individual species: a review. Tree Physiol. 30, 1192–1208.
Rodríguez, R., Espinosa, M., Real, P., Inzunza, J., 2002. Analysis of productivity of radiata pine plantations under different silvicultural regimes using the 3-PG process based model. Aust. For. 65, 165–172.
Roupsard, O., Ferhi, A., Granier, A., Pallo, F., Depommier, D., Mallet, B., Joly, H.I., Dreyer, E., 1999. Reverse phenology and dry-season water uptake by *Faidherbia albida* (Del.) A. Chev. in an agroforestry parkland of Sudanese west Africa. Funct. Ecol. 13, 460–472.
Ryan, M.G., Binkley, D., Fownes, J.H., 1997. Age-related decline in forest productivity: pattern and process. Adv. Ecol. Res. 27, 213–262.
Sands, P. 2004a. Adaptation of 3-PG to novel species: guidelines for data collection and parameter assignment. Technical Report No.141. CRC for Sustainable Production Forestry, Hobart, 35.
Sands, P. 2004b. 3PGPJS vsn 2.4 – A User-Friendly Interface to 3-PG, the Landsberg and Waring Model of Forest Productivity. Technical Report No. 140. CRC for Sustainable Production Forestry, Hobart.
Sands, P. J., 2010. 3-PG_{PJS} user manual, 27.
Sands, P.J., Landsberg, J.J., 2002. Parameterisation of 3-PG for plantation grown *Eucalyptus globulus*. Forest Ecol. Manag. 163, 273–292.
Soares, J.V., Almeida, A.C., 2001. Modeling the water balance and soil water fluxes in a fast-growing *Eucalyptus* plantation in Brazil. J. Hydrol. 253, 130–147.
Stape, J.L., Binkley, D., Jacob, W.S., Takahashi, E.N., 2006. A twin-plot approach to determine nutrient limitation and potential productivity in *Eucalyptus* plantations at landscape scales in Brazil. Forest Ecol. Manag. 223, 358–362.
Tang, R., Tang, J., Huang, L., 2014. Cyclobalanopsis glauca cultivation technolgy. Mod. Gard. 22, 043.
Tang, X., Estimation of biomass, volume and growth of subtropical forests in Shitai County, China, 2015, PhD Dissertation, Georg-August-Universität Göttingen, Göttingen.
Tang, X., Lu, Y., Fehrmann, L., Forrester, D. I., Guisasola, R., Pérez-Cruzado, C., Kleinn, C., in review. Estimation of stand-level aboveground biomass dynamics using tree ring analysis in a Chinese fir plantation in Shitai County, Anhui Province, China. New Forests.
Vanclay, J.K., Skovsgaard, J.P., 1997. Evaluating forest growth models. Ecol. Model. 98, 1–12.
Vertessy, R.A., Hatton, T.J., Benyon, R.G., Dawes, W.R., 1996. Long-term growth and water balance predictions for a mountain ash (*Eucalyptus regnans*) forest catchment subject to clear-felling and regeneration. Tree Physiol. 16, 221–232.
Wallace, J.S., 1997. Evaporation and radiation interception by neighbouring plants. Q. J. R. Meteorol. Soc. 123, 1885–1905.

Wang, W., Peng, C., Zhang, S.Y., Zhou, X., Larocque, G.R., Kneeshaw, D.D., Lei, X., 2011. Development of TRIPLEX-Management model for simulating the response of forest growth to pre-commercial thinning. Ecol. Model. 222, 2249–2261.

Waring, R.H., Landsberg, J.J., Williams, M., 1998. Net primary production of forests: a constant fraction of gross primary production. Tree Physiol. 18, 129–134.

Wei, L., Marshall, J.D., Zhang, J., Zhou, H., Powers, R.F., 2014a. 3-PG simulations of young ponderosa pine plantations under varied management intensity: Why do they grow so differently? Forest Ecol. Manag. 313, 69–82.

Wei, L., Marshall, J.D., Link, T.E., Kavanagh, K.L., Du, E., Pangle, R.E., Gag, P.J., Ubierna, N., 2014b. Constraining 3-PG with a new $\delta^{13}C$ submodel: a test using the $\delta^{13}C$ of tree rings. Plant Cell Environ. 37, 82–100.

Weiskittel, A.R., Maguire, D.A., Monserud, R.A., Johnson, G.P., 2010. A hybrid model for intensively managed Douglas-fir plantations in the Pacific Northwest, USA. Eur. J. Forest Res. 129, 325–338.

Xenakis, G., Ray, D., Mencuccini, M., 2008. Sensitivity and uncertainty analysis from a coupled 3-PG and soil organic matter decomposition model. Ecol. Model. 219, 1–16.

Xiang, W., Liu, S., Deng, X., Shen, A., Lei, X., Tian, D., Zhao, M., Peng, C., 2011. General allometric equations and biomass allocation of *Pinus massoniana* trees on a regional scale in southern China. Ecol. Res. 26, 697–711.

Xiao, Q., McPherson, E.G., 2011. Rainfall interception of three trees in Oakland, California. Urban Ecosyst. 14, 755–769.

Xu, X.N., Wang, Q., Hirata, E., 2005. Precipitation partitioning and related nutrient fluxes in a subtropical forest in Okinawa, Japan. Ann. Forest Sci. 62, 245–252.

Zeng, W.-S., 2015. Using nonlinear mixed model and dummy variable model approaches to develop origin-based individual tree biomass equations. Trees 29, 275–283.

Zhang, J., Liu, Y., Wu, C., et al., 2013. Litterfall production and dynamics of its decomposition of *Liquidambar formosana* plantation. Acta Agric. Univ. Jiangxiensis 35, 1187–1192.

Zhang, X., Deng, W., 2009. Efficient silviculture technology of *Castanopsis sclerophylla*. Mod. Agric. Sci. Technol. 5, 33 (in Chinese).

Zhao, M., Xiang, W., Peng, C., Tian, D., 2009. Simulating age-related changes in carbon storage and allocation in a Chinese fir plantation growing in southern China using the 3-PG model. Forest Ecol. Manag. 257, 1520–1531.

Zhou, J., Gao, L., 1985. Silviculture technology of excellent broadleaf trees. Zhejiang Science Press, Hangzhou (in Chinese) ⟨http://www.lhnw.gov.cn/member/linte/ycl/fx.htm⟩.